

Deep Restricted Kernel Machines Using Conjugate Feature Duality

Johan A. K. Suykens

johan.suykens@esat.kuleuven.be

KU Leuven ESAT-STADIUS, B-3001 Leuven, Belgium

The aim of this letter is to propose a theory of deep restricted kernel machines offering new foundations for deep learning with kernel machines. From the viewpoint of deep learning, it is partially related to restricted Boltzmann machines, which are characterized by visible and hidden units in a bipartite graph without hidden-to-hidden connections and deep learning extensions as deep belief networks and deep Boltzmann machines. From the viewpoint of kernel machines, it includes least squares support vector machines for classification and regression, kernel principal component analysis (PCA), matrix singular value decomposition, and Parzen-type models. A key element is to first characterize these kernel machines in terms of so-called conjugate feature duality, yielding a representation with visible and hidden units. It is shown how this is related to the energy form in restricted Boltzmann machines, with continuous variables in a nonprobabilistic setting. In this new framework of so-called restricted kernel machine (RKM) representations, the dual variables correspond to hidden features. Deep RKM are obtained by coupling the RKMs. The method is illustrated for deep RKM, consisting of three levels with a least squares support vector machine regression level and two kernel PCA levels. In its primal form also deep feedforward neural networks can be trained within this framework.

1 Introduction ---

Deep learning has become an important method of choice in several research areas including computer vision, speech recognition, and language processing (LeCun, Bengio, & Hinton, 2015). Among the existing techniques in deep learning are deep belief networks, deep Boltzmann machines, convolutional neural networks, stacked autoencoders with pre-training and fine-tuning, and others (Bengio, 2009; Goodfellow, Bengio, & Courville, 2016; Hinton, 2005; Hinton, Osindero, & Teh, 2006; LeCun et al., 2015; Lee, Grosse, Ranganath, & Ng, 2009; Salakhutdinov, 2015; Schmidhuber, 2015; Srivastava & Salakhutdinov, 2014; Chen, Schwing, Yuille, & Urtasun, 2015; Jaderberg, Simonyan, Vedaldi, & Zisserman, 2014; Schwing & Urtasun, 2015; Zheng et al., 2015). Support vector machines (SVM) and

kernel-based methods have made a large impact on a wide range of application fields, together with finding strong foundations in optimization and learning theory (Boser, Guyon, & Vapnik, 1992; Cortes & Vapnik, 1995; Rasmussen & Williams, 2006; Schölkopf & Smola, 2002; Suykens, Van Gestel, De Brabanter, De Moor, & Vandewalle, 2002; Vapnik, 1998; Wahba, 1990). Therefore, one can pose the question: Which synergies or common foundations could be developed between these different directions? There has already been exploration of such synergies—for example, in kernel methods for deep learning (Cho & Saul, 2009), deep gaussian processes (Damianou & Lawrence, 2013; Salakhutdinov & Hinton, 2007), convolutional kernel networks (Mairal, Koniusz, Harchaoui, & Schmid, 2014), multilayer support vector machines (Wiering & Schomaker, 2014), and mathematics of the neural response (Smale, Rosasco, Bouvrie, Caponnetto, & Poggio, 2010), among others.

In this letter, we present a new theory of deep restricted kernel machines (deep RKM), offering foundations for deep learning with kernel machines. It partially relates to restricted Boltzmann machines (RBMs), which are used within deep belief networks (Hinton, 2005; Hinton et al., 2006). In RBMs, one considers a specific type of Markov random field, characterized by a bipartite graph consisting of a layer of visible units and another layer of hidden units (Bengio, 2009; Fisher & Igel, 2014; Hinton et al., 2006; Salakhutdinov, 2015). In RBMs, which are related to harmoniums (Smolensky, 1986; Welling, Rosen-Zvi, & Hinton, 2004), there are no connections between the hidden units (Hinton, 2005), and often also no visible-to-visible connections. In deep belief networks, the hidden units of a layer are mapped to a next layer in order to create a deep architecture. In RBM, one considers stochastic binary variables (Ackley, Hinton, & Sejnowski, 1985; Hertz, Krogh, & Palmer, 1991), and extensions have been made to gaussian-Bernoulli variants (Salakhutdinov, 2015). Hopfield networks (Hopfield, 1982) take continuous values, and a class of Hamiltonian neural networks has been studied in DeWilde (1993). Also, discriminative RBMs have been studied where the class labels are considered at the level of visible units (Fisher & Igel, 2014; Larochelle & Bengio, 2008). In all of these methods the energy function plays an important role, as it also does in energy-based learning methods (LeCun, Chopra, Hadsell, Ranzato, & Huang, 2006).

Representation learning issues are considered to be important in deep learning (Bengio, Courville, & Vincent, 2013). The method proposed in this letter makes a link to restricted Boltzmann machines by characterizing several kernel machines by means of so-called conjugate feature duality. Duality is important in the context of support vector machines (Boser et al., 1992; Cortes & Vapnik, 1995; Vapnik, 1998; Suykens et al., 2002; Suykens, Alzate, & Pelckmans, 2010), optimization (Boyd & Vandenberghe, 2004; Rockafellar, 1987), and in mathematics and physics in general. Here we consider hidden features conjugated to part of the unknown variables. This part of

the formulation is linked to a restricted Boltzmann machine energy expression, though with continuous variables in a nonprobabilistic setting. In this way, a model can be expressed in both its primal representation and its dual representation and give an interpretation in terms of visible and hidden units, in analogy with RBM. The primal representation contains the feature map, while the dual model representation is expressed in terms of the kernel function and the conjugated features.

The class of kernel machines discussed in this letter includes least squares support vector machines (LS-SVM) for classification and regression, kernel principal component analysis (kernel PCA), matrix singular value decomposition (matrix SVD), and Parzen-type models. These have been previously conceived within a primal and Lagrange dual setting in Suykens and Vandewalle (1999b), Suykens et al. (2002), Suykens, Van Gestel, Vandewalle, and De Moor (2003), and Suykens (2013, 2016). Other examples are kernel spectral clustering (Alzate & Suykens, 2010; Mall, Langone, & Suykens, 2014), kernel canonical correlation analysis (Suykens et al., 2002), and several others, which will not be addressed in this letter, but can be the subject of future work. In this letter, we give a different characterization for these models, based on a property of quadratic forms, which can be verified through the Schur complement form. The property relates to a specific case of Legendre-Fenchel duality (Rockafellar, 1987). Also note that in classical mechanics, converting a Lagrangian into Hamiltonian formulation is by Legendre transformation (Goldstein, Poole, & Safko, 2002).

The kernel machines with conjugate feature representations are used then as building blocks to obtain the deep RKM by coupling the RKMs. The deep RKM becomes unrestricted after coupling the RKMs. The approach is explained for a model with three levels, consisting of two kernel PCA levels and a level with LS-SVM classification or regression. The conjugate features of level 1 are taken as input of level 2 and, subsequently, the features of level 2 as input for level 3. The objective of the deep RKM is the sum of the objectives of the RKMs in the different levels. The characterization of the stationary points leads to solving a set of nonlinear equations in the unknowns, which is computationally expensive. However, for the case of linear kernels, in part of the levels it reveals how kernel fusion is taking place over the different levels. For this case, a heuristic algorithm is obtained with level-wise solving. For the general nonlinear case, a reduced-set algorithm with estimation in the primal is proposed.

In this letter, we make a distinction between levels and layers. We use the terminology of levels to indicate the depth of the model. The terminology of *layers* is used here in connection to the feature map. Suykens and Vandewalle (1999a) showed how a multilayer perceptron can be trained by a support vector machine method. It is done by defining the hidden layer to be equal to the feature map. In this way, the hidden layer is treated at the feature map and the kernel parameters level. Suykens et al. (2002) explained that in SVM and LS-SVM models, one can have a neural networks

interpretation in both the primal and the dual. The number of hidden units in the primal equals the dimension of the feature space, while in the dual representation, it equals the number of support vectors. In this way, it provides a setting to work with parametric models in the primal and kernel-based models in the dual. Therefore, we also illustrate in this letter how deep multilayer feedforward neural networks can be trained within the deep RKM framework. While in classical backpropagation (Rumelhart, Hinton, & Williams, 1986), one typically learns the model by specifying a single objective (e.g., unless imposing additional stability constraints to obtain stable multilayer recurrent networks with dynamic backpropagation; (Suykens, Vandewalle, & De Moor, 1995), in the deep RKM the objective function consists of the different objectives related to the different levels.

In summary, we aim at contributing to the following challenging questions in this letter:

- Can we find new synergies and foundations between SVM and kernel methods and deep learning architectures?
- Can we extend primal and dual model representations, as occurring in SVM and LS-SVM models, from shallow to deep architectures?
- Can we handle deep feedforward neural networks and deep kernel machines within a common setting?

In order to address these questions, this letter is organized as follows. Section 2 outlines the context of this letter with a brief introductory part on restricted Boltzmann machines, SVMs, LS-SVMs, kernel PCA, and SVD. In section 3 we explain how these kernel machines can be characterized by conjugate feature duality with visible and hidden units. In section 4 deep restricted kernel machines are explained for three levels: an LS-SVM regression level and two additional kernel PCA levels. In section 5, different algorithms are proposed for solving in either the primal or the dual, where the former will be related to deep feedforward neural networks and the latter to kernel-based models. Illustrations with numerical examples are given in section 6. Section 7 concludes the letter.

2 Preliminaries and Context

In this section, we explain basic principles of restricted Boltzmann machines, SVMs, LS-SVMs, and related formulations for kernel PCA, and SVD. These are basic ingredients needed before introducing restricted kernel machines in section 3.

2.1 Restricted Boltzmann Machines. An RBM is a specific type of Markov random field, characterized by a bipartite graph consisting of a layer of visible units and another layer of hidden units (Bengio, 2009; Fisher & Igel, 2014; Hinton et al., 2006; Salakhutdinov, 2015), without hidden-to-hidden connections. Both the visible and hidden variables, denoted by v

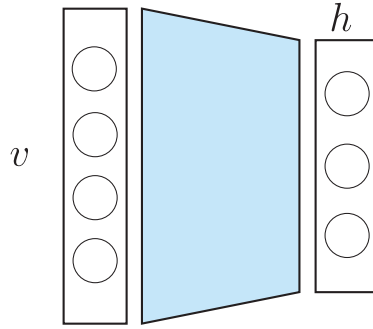


Figure 1: Restricted Boltzmann machine consisting of a layer of visible units v and a layer of hidden units h . They are interconnected through the interaction matrix W , depicted in blue.

and h , respectively, have stochastic binary units with value 0 or 1. A joint state $\{v, h\}$ is defined for these visible and hidden variables with energy (see Figure 1),

$$E(v, h; \theta) = -v^T W h - c^T v - a^T h, \tag{2.1}$$

where $\theta = \{W, c, a\}$ are the model parameters, W is an interaction weight matrix, and c, a contain bias terms.

One then obtains the joint distribution over the visible and hidden units as

$$P(v, h; \theta) = \frac{1}{Z(\theta)} \exp(-E(v, h; \theta)) \tag{2.2}$$

with the partition function

$$Z(\theta) = \sum_v \sum_h \exp(-E(v, h; \theta))$$

for normalization.

Thanks to the specific bipartite structure, one can obtain an explicit expression for the marginalization $P(v; \theta) = \frac{1}{Z(\theta)} \sum_h \exp(-E(v, h; \theta))$. The conditional distributions are obtained as

$$\begin{aligned} P(h|v; \theta) &= \prod_j p(h_j|v), \\ P(v|h; \theta) &= \prod_i p(v_i|h), \end{aligned} \tag{2.3}$$

where $p(h_{(j)} = 1|v) = \sigma(\sum_i W_{ij}v_{(i)} + a_j)$ and $p(v_{(i)} = 1|h) = \sigma(\sum_j W_{ij}h_{(j)} + d_i)$ with $\sigma(x) = 1/(1 + \exp(-x))$ the logistic function. Here $v_{(i)}$ and $h_{(j)}$ denote the i th visible unit and the j th hidden unit, respectively.

Because exact maximum likelihood for this model is intractable, a contrastive divergence algorithm is used with the following update equation for the weights,

$$\Delta W = \alpha(\mathbb{E}_{P_{\text{data}}}(vh^T) - \mathbb{E}_{P_T}(vh^T)), \tag{2.4}$$

with learning rate α and $\mathbb{E}_{P_{\text{data}}}$ the expectation with regard to the data distribution $P_{\text{data}}(h, v; \theta) = P(h|v; \theta)P_{\text{data}}(v)$, where $P_{\text{data}}(v)$ denotes the empirical distribution. Furthermore, \mathbb{E}_{P_T} is a distribution defined by running a Gibbs chain for T steps initialized at the data. Often one takes $T = 1$, while $T \rightarrow \infty$ recovers the maximum likelihood approach (Salakhutdinov, 2015).

In Boltzmann machines there are, in addition to visible-to-hidden, also visible-to-visible and hidden-to-hidden interaction terms with

$$E(v, h; \theta) = -v^T W h - \frac{1}{2} v^T L v - \frac{1}{2} h^T G h \tag{2.5}$$

and $\theta = \{W, L, G\}$ as explained in Salakhutdinov and Hinton (2009).

In section 3 we make a connection between the energy expression, equation 2.1, and a new representation of least squares support vector machines and related kernel machines, which will be made in terms of visible and hidden units. We now briefly review basics of SVMs, LS-SVMs, PCA, and SVD.

2.2 Least Squares Support Vector Machines and Related Kernel Machines.

2.2.1 SVM and LS-SVM. Assume a binary classification problem with training data $\{(x_i, y_i)\}_{i=1}^N$ with input data $x_i \in \mathbb{R}^d$ and corresponding class labels $y_i \in \{-1, 1\}$. An SVM classifier takes the form

$$\hat{y} = \text{sign}[w^T \varphi(x) + b],$$

where the feature map $\varphi(\cdot) : \mathbb{R}^d \rightarrow \mathbb{R}^{n_f}$ maps the data from the input space to a high-dimensional feature space and \hat{y} is the estimated class label for a given input point $x \in \mathbb{R}^d$. The training problem for this SVM classifier (Boser et al., 1992; Cortes & Vapnik, 1995; Vapnik, 1998) is

$$\begin{aligned}
 \min_{w,b,\xi} \quad & \frac{1}{2} w^T w + c \sum_{i=1}^N \xi_i \\
 \text{subject to} \quad & y_i [w^T \varphi(x_i) + b] \geq 1 - \xi_i, \quad i = 1, \dots, N \\
 & \xi_i \geq 0, \quad i = 1, \dots, N,
 \end{aligned} \tag{2.6}$$

where the objective function makes a trade-off between minimization of the regularization term (corresponding to maximization of the margin $2/\|w\|_2$) and the amount of misclassifications, controlled by the regularization constant $c > 0$. The slack variables ξ_i are needed to tolerate misclassifications on the training data in order to avoid overfitting the data. The following dual problem in the Lagrange multipliers α_i is obtained, related to the first set of constraints:

$$\begin{aligned}
 \max_{\alpha} \quad & -\frac{1}{2} \sum_{i,j=1}^N y_i y_j K(x_i, x_j) \alpha_i \alpha_j + \sum_{j=1}^N \alpha_j \\
 \text{subject to} \quad & \sum_{i=1}^N \alpha_i y_i = 0 \\
 & 0 \leq \alpha_i \leq c, \quad i = 1, \dots, N.
 \end{aligned} \tag{2.7}$$

Here a positive-definite kernel K is used with $K(x, z) = \varphi(x)^T \varphi(z) = \sum_{j=1}^{n_f} \varphi_j(x) \varphi_j(z)$. The SVM classifier is expressed in the dual as

$$\hat{y} = \text{sign} \left[\sum_{i \in \mathcal{S}_{SV}} \alpha_i y_i K(x_i, x) + b \right], \tag{2.8}$$

where \mathcal{S}_{SV} denotes the set of support vectors, corresponding to the nonzero α_i values. Common choices are, for example, to take a linear $K(x_i, x_j) = x_i^T x_j$, polynomial $K(x_i, x_j) = (\nu + x_i^T x_j)^d$ with $\nu \geq 0$, or gaussian RBF kernel $K(x_i, x_j) = \exp(-\|x_i - x_j\|_2^2 / \sigma^2)$.

The LS-SVM classifier (Suykens & Vandewalle, 1999b) is a modification to it,

$$\begin{aligned}
 \min_{w,b,e_i} \quad & \frac{1}{2} w^T w + \gamma \frac{1}{2} \sum_{i=1}^N e_i^2 \\
 \text{subject to} \quad & y_i [w^T \varphi(x_i) + b] = 1 - e_i, \quad i = 1, \dots, N,
 \end{aligned} \tag{2.9}$$

where the value 1 in the constraints is taken as a target value instead of a threshold value. This implicitly corresponds to a regression on the

class labels ± 1 . From the Lagrangian $\mathcal{L}(w, b, e; \alpha) = \frac{1}{2}w^T w + \gamma \frac{1}{2} \sum_{i=1}^N e_i^2 - \sum_{i=1}^N \alpha_i \{y_i [w^T \varphi(x_i) + b] - 1 + e_i\}$, one takes the conditions for optimality $\partial \mathcal{L} / \partial w = 0, \partial \mathcal{L} / \partial b = 0, \partial \mathcal{L} / \partial e_i = 0, \partial \mathcal{L} / \partial \alpha_i = 0$. Writing the solution in α, b gives the square linear system

$$\left[\begin{array}{c|c} \Omega + I/\gamma & y_{1:N} \\ \hline y_{1:N}^T & 0 \end{array} \right] \begin{bmatrix} \alpha \\ b \end{bmatrix} = \begin{bmatrix} 1_N \\ 0 \end{bmatrix}, \tag{2.10}$$

where $\Omega_{ij} = y_i y_j \varphi(x_i)^T \varphi(x_j) = y_i y_j K(x_i, x_j)$ and $y_{1:N} = [y_1; \dots; y_N]$, $1_N = [1; \dots; 1]$ with, as classifier in the dual,

$$\hat{y} = \text{sign} \left[\sum_{i=1}^N \alpha_i y_i K(x_i, x) + b \right]. \tag{2.11}$$

This formulation has also been extended to multiclass problems in Suykens et al. (2002).

In the LS-SVM regression formulation (Suykens et al., 2002) one performs ridge regression in the feature space with an additional bias term b ,

$$\begin{aligned} \min_{w, b, e_i} \quad & \frac{1}{2} w^T w + \gamma \frac{1}{2} \sum_{i=1}^N e_i^2 \\ \text{subject to} \quad & y_i = w^T \varphi(x_i) + b + e_i, \quad i = 1, \dots, N, \end{aligned} \tag{2.12}$$

which gives

$$\left[\begin{array}{c|c} K + I/\gamma & 1_N \\ \hline 1_N^T & 0 \end{array} \right] \begin{bmatrix} \alpha \\ b \end{bmatrix} = \begin{bmatrix} y_{1:N} \\ 0 \end{bmatrix} \tag{2.13}$$

with the predicted output

$$\hat{y} = \sum_{i=1}^N \alpha_i K(x_i, x) + b, \tag{2.14}$$

where $K_{ij} = K(x_i, x_j) = \varphi(x_i)^T \varphi(x_j)$. The classifier formulation can also be transformed into the regression formulation by multiplying the constraints in equation 2.9 by the class labels and considering new error variables (Suykens et al., 2002). In the zero bias term case, this corresponds to kernel ridge regression (Saunders, Gammerman, & Vovk, 1998), which is also

related to function estimation in reproducing kernel Hilbert spaces, regularization networks, and gaussian processes, within a different setting (Poggio & Girosi, 1990; Wahba, 1990; Rasmussen & Williams, 2006; Suykens et al., 2002).

2.2.2 Kernel PCA and Matrix SVD. Within the setting of using equality constraints and the L_2 loss function, typical for LS-SVMs, one can characterize the kernel PCA problem (Schölkopf, Smola, & Müller, 1998) as follows, as shown in Suykens et al. (2002, 2003):

$$\begin{aligned} \min_{w,b,e_i} \quad & \frac{1}{2} w^T w - \gamma \frac{1}{2} \sum_{i=1}^N e_i^2 \\ \text{subject to} \quad & e_i = w^T \varphi(x_i) + b, \quad i = 1, \dots, N. \end{aligned} \tag{2.15}$$

From the KKT conditions, one obtains the following in the Lagrange multipliers α_i ,

$$K^{(c)} \alpha = \lambda \alpha \quad \text{with} \quad \lambda = 1/\gamma, \tag{2.16}$$

where $K_{ij}^{(c)} = (\varphi(x_i) - \hat{\mu}_\varphi)^T (\varphi(x_j) - \hat{\mu}_\varphi)$ are the elements of the centered kernel matrix $K^{(c)}$, $\hat{\mu}_\varphi = (1/N) \sum_{i=1}^N \varphi(x_i)$ and $\alpha = [\alpha_1; \dots; \alpha_N]$. In equation 2.15, maximizing instead of minimizing also leads to equation 2.16. The centering of the kernel matrix is obtained as a result of taking a bias term b in the model. The γ value is treated at a selection level and is chosen so as to correspond to $\lambda = 1/\gamma$, where λ are eigenvalues of $K^{(c)}$. In the zero bias term case, $K^{(c)}$ becomes the kernel matrix $K = [\varphi(x_i)^T \varphi(x_j)]$. Also, kernel spectral clustering (Alzate & Suykens, 2010) was obtained in this setting by considering a weighted version of the L_2 loss part, weighted by the inverse of the degree matrix of the graph in the clustering problem.

Suykens (2016) showed recently that matrix SVD can be obtained from the following primal problem:

$$\begin{aligned} \min_{w,v,e_i,r} \quad & -w^T v + \gamma \frac{1}{2} \sum_{i=1}^N e_i^2 + \gamma \frac{1}{2} \sum_{j=1}^M r_j^2 \\ \text{subject to} \quad & e_i = w^T \varphi(x_i), \quad i = 1, \dots, N \\ & r_j = v^T \psi(z_j), \quad j = 1, \dots, M, \end{aligned} \tag{2.17}$$

where $\{x_i\}_{i=1}^N$ and $\{z_j\}_{j=1}^M$ are data sets related to two data sources, which in the matrix SVD (Golub & Van Loan, 1989; Stewart, 1993) case correspond to the sets of rows and columns of the given matrix. Here one has two feature maps $\varphi(\cdot)$ and $\psi(\cdot)$. After taking the Lagrangian and the necessary

conditions for optimality, the dual problem in the Lagrange multipliers α_i and β_j , related to the first and second set of constraints, results in

$$\begin{bmatrix} 0 & A \\ A^T & 0 \end{bmatrix} \begin{bmatrix} \alpha \\ \beta \end{bmatrix} = \lambda \begin{bmatrix} \alpha \\ \beta \end{bmatrix}, \tag{2.18}$$

where $A = [\varphi(x_i)^T \psi(z_j)]$ denotes the matrix with ij th entry $\varphi(x_i)^T \psi(z_j)$, $\lambda = 1/\gamma$ corresponding to nonzero eigenvalues, and $\alpha = [\alpha_1; \dots; \alpha_N]$, $\beta = [\beta_1; \dots; \beta_M]$. For a given matrix A , by choosing the linear feature maps $\varphi(x_i) = C^T x_i$, $\psi(z_j) = z_j$ with a compatibility matrix C that satisfies $ACA = A$, this eigenvalue problem corresponds to the SVD of matrix A (Suykens, 2016) in connection with Lanczos’s decomposition theorem. One can also see that for a symmetric matrix, the two data sources coincide, and the objective of equation 2.17 reduces to the kernel PCA objective, equation 2.15 (Suykens, 2016), involving only one feature map instead of two feature maps.

3 Restricted Kernel Machines and Conjugate Feature Duality

3.1 LS-SVM Regression as a Restricted Kernel Machine: Linear Case.

A training data set $\mathcal{D} = \{(x_i, y_i)\}_{i=1}^N$ is assumed to be given with input data $x_i \in \mathbb{R}^d$ and output data $y_i \in \mathbb{R}^p$ (now with p outputs), where the data are assumed to be identical and independently distributed and drawn from an unknown but fixed underlying distribution $P(x,y)$, a common assumption made in statistical learning theory (Vapnik, 1998).

We will explain now how LS-SVM regression can be linked to the energy form expression of an RBM with an interpretation in terms of hidden and visible units. In view of these connections with RBMs and the fact that there will be no hidden-to-hidden connections, we will call it a restricted kernel machine (RKM) representation, when this particular interpretation of the model is made. For LS-SVM regression, the part in the RKM interpretation that will take a similar form as the RBM energy function is

$$\begin{aligned} R_{\text{RKM}}(v, h) &= -v^T \tilde{W}h \\ &= -(x^T W h + b^T h - y^T h) \\ &= e^T h, \end{aligned} \tag{3.1}$$

with a vector of hidden units $h \in \mathbb{R}^p$ and a vector of visible units $v \in \mathbb{R}^{n_v}$ with $n_v = d + 1 + p$ equal to

$$v = \begin{bmatrix} x \\ 1 \\ -y \end{bmatrix} \text{ and } \tilde{W} = \begin{bmatrix} W \\ b^T \\ I_p \end{bmatrix}, \tag{3.2}$$

and $e = y - \hat{y}$ with $\hat{y} = W^T x + b$ the estimated output vector for a given input vector x where $e, y, \hat{y} \in \mathbb{R}^p, W \in \mathbb{R}^{d \times p}, b \in \mathbb{R}^p$. Note that b is treated as part of the interconnection matrix by adding a constant 1 within the vector v , which is also frequently done in the area of neural networks (Suykens et al., 1995). While in RBM the units are binary valued, in the RKM, they are continuous valued. The notation R in $R_{\text{RKM}}(v, h)$ refers to the fact that the expression is restricted; there are no hidden-to-hidden connections.

For the training problem, the sum is taken over the training data $\{(x_i, y_i)\}_{i=1}^N$ with

$$\begin{aligned} R_{\text{RKM}}^{\text{train}} &= \sum_{i=1}^N R_{\text{RKM}}(v_i, h_i) \\ &= - \sum_{i=1}^N (x_i^T W h_i + b^T h_i - y_i^T h_i) \\ &= \sum_{i=1}^N e_i^T h_i. \end{aligned} \tag{3.3}$$

Note that we will adopt the following notation $h_{(j),i}$ to denote the value of the j th unit for the i th data point, and $e_i, h_i \in \mathbb{R}^p$ for $i = 1, \dots, N$.

We start now from the LS-SVM regression training problem, equation 2.12, but for the multiple outputs case. We express the objective in terms of $R_{\text{RKM}}^{\text{train}}$ and show how the hidden units can be introduced. Defining $\lambda = 1/\gamma > 0$, we obtain

$$\begin{aligned} J &= \frac{\eta}{2} \text{Tr}(W^T W) + \frac{1}{2\lambda} \sum_{i=1}^N e_i^T e_i \text{ s.t. } e_i = y_i - W^T x_i - b, \forall i \\ &\geq \sum_{i=1}^N e_i^T h_i - \frac{\lambda}{2} \sum_{i=1}^N h_i^T h_i + \frac{\eta}{2} \text{Tr}(W^T W) \text{ s.t. } e_i = y_i - W^T x_i - b, \forall i \\ &= \sum_{i=1}^N (y_i^T - x_i^T W - b^T) h_i - \frac{\lambda}{2} \sum_{i=1}^N h_i^T h_i + \frac{\eta}{2} \text{Tr}(W^T W) \triangleq \underline{J} \\ &= R_{\text{RKM}}^{\text{train}} - \frac{\lambda}{2} \sum_{i=1}^N h_i^T h_i + \frac{\eta}{2} \text{Tr}(W^T W), \end{aligned} \tag{3.4}$$

where λ, η are positive regularization constants and the first term corresponds to $R_{\text{RKM}}^{\text{train}}$. J denotes the lower bound on J .¹ This is based on the property that for two arbitrary vectors e, h , one has

$$\frac{1}{2\lambda}e^T e \geq e^T h - \frac{\lambda}{2}h^T h, \quad \forall e, h \in \mathbb{R}^p. \tag{3.5}$$

The maximal value of the right-hand side in equation 3.5 is obtained for $h = e/\lambda$, which follows from $\partial(e^T h - \frac{\lambda}{2}h^T h)/\partial h = 0$ and $\partial^2(e^T h - \frac{\lambda}{2}h^T h)/\partial h^2 = -\lambda I < 0$. The maximal value that can be obtained for the right-hand side equals the left-hand side, $\frac{1}{2\lambda}e^T e$. The property 3.5 can also be verified by writing it in quadratic form,

$$\frac{1}{2} \begin{bmatrix} e^T & h^T \end{bmatrix} \begin{bmatrix} \frac{1}{\lambda} I & I \\ I & \lambda I \end{bmatrix} \begin{bmatrix} e \\ h \end{bmatrix} \geq 0, \quad \forall e, h \in \mathbb{R}^p, \tag{3.6}$$

which holds. This follows immediately from the Schur complement form,² which results in the condition $\frac{1}{2}(\lambda I - I(\lambda I)I) \geq 0$, which holds. Writing equation 3.5 as

$$\frac{1}{2\lambda}e^T e + \frac{\lambda}{2}h^T h \geq e^T h \tag{3.7}$$

gives a property that is also known in Legendre-Fenchel duality for the case of a quadratic function (Rockafellar, 1987). Furthermore, it also follows from equation 3.5 that

$$\frac{1}{2\lambda}e^T e = \max_h \left(e^T h - \frac{\lambda}{2}h^T h \right). \tag{3.8}$$

We will call the method of introducing the hidden features h_i into equation 3.4 *conjugate feature duality*, where the hidden features h_i are conjugated to the e_i . Here, $R_{\text{RKM}}^{\text{train}} = \sum_i e_i^T h_i$ will be called an *inner pairing* between the e_i and the hidden features h_i (see Figure 2).

¹Note that also the term $-\frac{\lambda}{2} \sum_{i=1}^N h_i^T h_i$ appears. This would in a Boltzmann machine energy correspond to matrix G equal to the identity matrix. The term $\frac{\eta}{2} \text{Tr}(W^T W)$ is an additional regularization term.

²This states that for a matrix $Q = \begin{bmatrix} A & B \\ B^T & C \end{bmatrix}$, one has $Q \geq 0$ if and only if $A > 0$ and the Schur complement $C - B^T A^{-1} B \geq 0$ (Boyd & Vandenberghe, 2004).

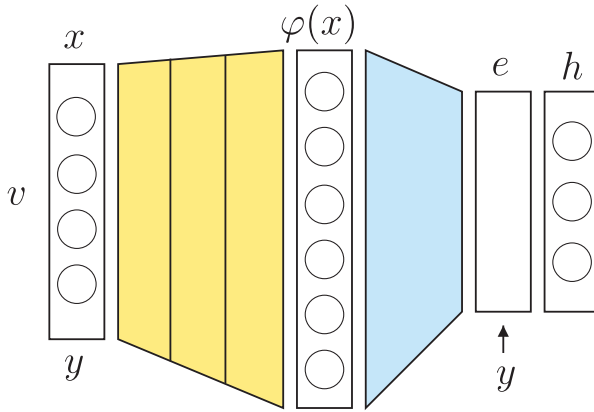


Figure 2: Restricted kernel machine (RKM) representation for regression. The feature map $\varphi(x)$ maps the input vector x to a feature space (possibly by multilayers, depicted in yellow), and the hidden features are obtained through an inner pairing $e^T h$ where $e = y - \hat{y}$ compares the given output vector y with the predictive model output vector $\hat{y} = W^T \varphi(x) + b$, where the interconnection matrix W is depicted in blue.

We proceed now by looking at the stationary points of $J(h_i, W, b)$:³

$$\begin{cases} \frac{\partial J}{\partial h_i} = 0 \Rightarrow y_i = W^T x_i + b + \lambda h_i, \quad \forall i \\ \frac{\partial J}{\partial W} = 0 \Rightarrow W = \frac{1}{\eta} \sum_i x_i h_i^T \\ \frac{\partial J}{\partial b} = 0 \Rightarrow \sum_i h_i = 0. \end{cases} \tag{3.9}$$

The first condition yields $h_i = e_i/\lambda$, which means that the maximal value of J is reached. Therefore, $y_i = \hat{y}_i + e_i = \hat{y}_i + \lambda h_i$. Also note the similarity between the condition $W = \frac{1}{\eta} \sum_i x_i h_i^T$ and equation 2.4 in the contrastive divergence algorithm. Elimination of h_i from this set of conditions gives the solution in W, b :

³The following properties are used throughout this letter: $\frac{\partial \text{Tr}(X^T B X)}{\partial X} = B X + B^T X$, $\frac{\partial a^T X b}{\partial X} = a b^T$, $\frac{\partial a^T X^T b}{\partial X} = b a^T$, $\frac{\partial \text{Tr}(X^T A)}{\partial X} = A$, $\frac{\partial \text{Tr}(A X^T)}{\partial X} = A$, $\frac{\partial \text{Tr}(X A)}{\partial X} = A^T$, $\frac{\partial x^T a}{\partial x} = \frac{\partial a^T x}{\partial x} = a$, $a^T a = \text{Tr}(a a^T)$ for matrices A, B, X and vectors a, b (Petersen & Pedersen, 2012).

$$\left[\begin{array}{c|c} \sum_i x_i x_i^T + \lambda \eta I_d & \sum_i x_i \\ \hline \sum_i x_i^T & N \end{array} \right] \left[\begin{array}{c} W \\ b^T \end{array} \right] = \left[\begin{array}{c} \sum_i x_i y_i^T \\ \sum_i y_i \end{array} \right]. \tag{3.10}$$

Elimination of W from the set of conditions gives the solution in h_i, b :

$$\left[\begin{array}{c|c} \frac{1}{\eta} [x_i^T x_j] + \lambda I_N & 1_N \\ \hline 1_N^T & 0 \end{array} \right] \left[\begin{array}{c} H^T \\ b^T \end{array} \right] = \left[\begin{array}{c} Y^T \\ 0 \end{array} \right], \tag{3.11}$$

with $[x_i^T x_j]$ denoting the matrix with ij -entry $x_i^T x_j$, $H = [h_1 \dots h_N] \in \mathbb{R}^{p \times N}$, $Y = [y_1 \dots y_N] \in \mathbb{R}^{p \times N}$. From this square linear system, one can solve $\{h_i\}$ and b . 1_N denotes a vector of all ones of size N and I_N the identity matrix of size $N \times N$.

It is remarkable to see here that the hidden features h_i take the same role as the Lagrange dual variables α_i in the LS-SVM formulation based on Lagrange duality, equation 2.13, when taking $\eta = 1$ and $p = 1$. For the estimated values \hat{y}_i on the training data, one can express the model in terms of W, b or in terms of h_i, b . In the restricted kernel machine interpretation of the LS-SVM regression, one has the following primal and dual model representations:

$$\begin{array}{l} (P)_{\text{RKM}} : \hat{y} = W^T x + b \\ \nearrow \\ \mathcal{M} \\ \searrow \\ (D)_{\text{RKM}} : \hat{y} = \frac{1}{\eta} \sum_j h_j x_j^T x + b \end{array} \tag{3.12}$$

evaluated at a point x where the primal representation is in terms of W, b and the dual representation is in the hidden features h_i . The primal representation is suitable for handling the “large N , small d ” case, while the dual representation for “small N , large d ” (Suykens et al., 2002).

3.2 Nonlinear Case. The extension to the general nonlinear case goes by replacing x_i by $\varphi(x_i)$ where $\varphi(x_i) : \mathbb{R}^d \rightarrow \mathbb{R}^{n_f}$ denotes the feature map, with n_f the dimension of the feature space. Therefore, the objective function for, the RKM interpretation becomes

$$J = \sum_{i=1}^N (y_i^T - \varphi(x_i)^T W - b^T) h_i - \frac{\lambda}{2} \sum_{i=1}^N h_i^T h_i + \frac{\eta}{2} \text{Tr}(W^T W), \tag{3.13}$$

with the vector of visible units $v \in \mathbb{R}^{n_v}$ with $n_v = n_f + 1 + p$ equal to

$$v = \begin{bmatrix} \varphi(x) \\ 1 \\ -y \end{bmatrix}. \tag{3.14}$$

Following the same approach as in the linear case, one then obtains as a solution in the primal

$$\left[\begin{array}{c|c} \sum_j \varphi(x_j)\varphi(x_j)^T + \lambda\eta I_{n_f} & \sum_j \varphi(x_j) \\ \hline \sum_j \varphi(x_j)^T & N \end{array} \right] \begin{bmatrix} W \\ b^T \end{bmatrix} = \begin{bmatrix} \sum_j \varphi(x_j)y_j^T \\ \sum_j y_j^T \end{bmatrix}. \tag{3.15}$$

In the conjugate feature dual, one obtains the same linear system as equation 3.11, but with the positive-definite kernel $K(x_i, x_j) = \varphi(x_i)^T \varphi(x_j)$ instead of the linear kernel $x_i^T x_j$:

$$\left[\begin{array}{c|c} \frac{1}{\eta}K + \lambda I_N & 1_N \\ \hline 1_N^T & 0 \end{array} \right] \begin{bmatrix} H^T \\ b^T \end{bmatrix} = \begin{bmatrix} Y^T \\ 0 \end{bmatrix}. \tag{3.16}$$

We also employ the notation $[K(x_i, x_j)]$ to denote the kernel matrix K with the ij th entry equal to $K(x_i, x_j)$.

The primal and dual model representations are expressed in terms of the feature map and kernel function, respectively:

$$\begin{array}{l} (P)_{\text{RKM}} : \hat{y} = W^T \varphi(x) + b \\ \nearrow \\ \mathcal{M} \\ \searrow \\ (D)_{\text{RKM}} : \hat{y} = \frac{1}{\eta} \sum_j h_j K(x_j, x) + b. \end{array} \tag{3.17}$$

One can define the feature map in either an implicit or an explicit way. When employing a positive-definite kernel function $K(\cdot, \cdot)$, according to the Mercer theorem, there exists a feature map φ such that $K(x_i, x_j) = \varphi(x_i)^T \varphi(x_j)$ holds. On the other hand, one could also explicitly define an expression for φ and construct the kernel function according to $K(x_i, x_j) := \varphi(x_i)^T \varphi(x_j)$. For multilayer perceptrons, Suykens and Vandewalle (1999a) showed that the hidden layer can be chosen as the feature map. We can let it correspond to

$$\varphi_{\text{FF}}(x) = \sigma(U_q \sigma(\dots \sigma(U_2 \sigma(U_1 x + \beta_1) + \beta_2) \dots) + \beta_q) \tag{3.18}$$

related to a feedforward (FF) neural network with multilayers, with hidden layer matrices U_1, U_2, \dots, U_q and bias term vectors $\beta_1, \beta_2, \dots, \beta_q$. By construction, one obtains $K_{\text{FF}}(x_i, x_j) := \varphi_{\text{FF}}(x_i)^T \varphi_{\text{FF}}(x_j)$. Note that the activation function σ might be different also for each of the hidden layers. A common choice is a sigmoid or hyperbolic tangent function. Within the context of this letter, $U_1, \dots, U_q, \beta_1, \dots, \beta_q$ are treated at the feature map and the kernel parameter levels.

As Suykens et al. (2002) explained, one can also give a neural network interpretation to both the primal and the dual representation, with a number of hidden units equal to the dimension of the feature space for the primal representation and the number of support vectors in the dual representation, respectively. For the case of a gaussian RBF kernel, one has a one-hidden-layer interpretation with an infinite number of hidden units in the primal, while in the dual, the number of hidden units equals the number of support vectors.

3.3 Classifier Formulation. In the multiclass case, the LS-SVM classifier constraints are

$$D_{y_i}(W^T \varphi(x_i) + b) = 1_p - e_i, i = 1, \dots, N, \tag{3.19}$$

where $y_i \in \{-1, 1\}^p, e_i \in \mathbb{R}^p$ with p outputs encoding the classes and diagonal matrix $D_{y_i} = \text{diag}\{y_{(1),i}, \dots, y_{(p),i}\}$.

In this case, starting from the LS-SVM classifier objective, one obtains

$$\begin{aligned} J &= \frac{\eta}{2} \text{Tr}(W^T W) + \frac{1}{2\lambda} \sum_{i=1}^N e_i^T e_i \text{ s.t. } e_i = 1_p - D_{y_i}(W^T \varphi(x_i) + b), \forall i \\ &\geq \sum_{i=1}^N e_i^T h_i - \frac{\lambda}{2} \sum_{i=1}^N h_i^T h_i + \frac{\eta}{2} \text{Tr}(W^T W) \text{ s.t. } e_i = 1_p \\ &\quad - D_{y_i}(W^T \varphi(x_i) + b), \forall i \\ &= \sum_{i=1}^N \left(1_p^T - (\varphi(x_i)^T W + b^T) D_{y_i} \right) h_i - \frac{\lambda}{2} \sum_{i=1}^N h_i^T h_i + \frac{\eta}{2} \text{Tr}(W^T W) \triangleq \underline{J}. \end{aligned} \tag{3.20}$$

The stationary points of $\underline{J}(h_i, W, b)$ are given by

$$\begin{cases} \frac{\partial J}{\partial h_i} = 0 \Rightarrow 1_p = D_{y_i}(W^T \varphi(x_i) + b) + \lambda h_i, \quad \forall i \\ \frac{\partial J}{\partial W} = 0 \Rightarrow W = \frac{1}{\eta} \sum_i \varphi(x_i) h_i^T D_{y_i} \\ \frac{\partial J}{\partial b} = 0 \Rightarrow \sum_i D_{y_i} h_i = 0. \end{cases} \quad (3.21)$$

The solution in the conjugate features follows then from the linear system:

$$\left[\begin{array}{c|c} \frac{1}{\eta} K + \lambda I_N & 1_N \\ \hline 1_N^T & 0 \end{array} \right] \begin{bmatrix} H_D^T \\ b^T \end{bmatrix} = \begin{bmatrix} Y^T \\ 0 \end{bmatrix} \quad (3.22)$$

with $H_D = [D_{y_1} h_1, \dots, D_{y_N} h_N]$.

The primal and dual model representations are expressed in terms of the feature map and the kernel function, respectively:

$$\begin{array}{l} (P)_{\text{RKM}} : \hat{y} = \text{sign}[W^T \varphi(x) + b] \\ \nearrow \\ \mathcal{M} \\ \searrow \\ (D)_{\text{RKM}} : \hat{y} = \text{sign} \left[\frac{1}{\eta} \sum_j D_{y_j} h_j K(x_j, x) + b \right]. \end{array} \quad (3.23)$$

3.4 Kernel PCA. In the kernel PCA case we start from the objective in equation 2.15 and introduce the conjugate hidden features:

$$\begin{aligned} J &= \frac{\eta}{2} \text{Tr}(W^T W) - \frac{1}{2\lambda} \sum_{i=1}^N e_i^T e_i \quad \text{s.t. } e_i = W^T \varphi(x_i), \forall i \\ &\leq -\sum_{i=1}^N e_i^T h_i + \frac{\lambda}{2} \sum_{i=1}^N h_i^T h_i + \frac{\eta}{2} \text{Tr}(W^T W) \quad \text{s.t. } e_i = W^T \varphi(x_i), \forall i \\ &= -\sum_{i=1}^N \varphi(x_i)^T W h_i + \frac{\lambda}{2} \sum_{i=1}^N h_i^T h_i + \frac{\eta}{2} \text{Tr}(W^T W) \triangleq \bar{J} \\ &= -R_{\text{RKM}}^{\text{train}} + \frac{\lambda}{2} \sum_{i=1}^N h_i^T h_i + \frac{\eta}{2} \text{Tr}(W^T W), \end{aligned} \quad (3.24)$$

where the upper bound \bar{J} is introduced now by relying on the same property as used in the regression/classification case, $\frac{1}{2\lambda}e^T e + \frac{\lambda}{2}h^T h \geq e^T h$, but in a different way. Note that

$$-\frac{1}{2\lambda}e^T e = \min_h (-e^T h + \frac{\lambda}{2}h^T h). \tag{3.25}$$

The minimal value for the right-hand side is obtained for $h = e/\lambda$, which equals the left-hand side in that case.

We then proceed by characterizing the stationary points of $\bar{J}(h_i, W)$:

$$\begin{cases} \frac{\partial \bar{J}}{\partial h_i} = 0 \Rightarrow W^T \varphi(x_i) = \lambda h_i, \quad \forall i \\ \frac{\partial \bar{J}}{\partial W} = 0 \Rightarrow W = \frac{1}{\eta} \sum_i \varphi(x_i) h_i^T. \end{cases} \tag{3.26}$$

Note that the first condition yields $h_i = e_i/\lambda$. Therefore, the minimum value of \bar{J} is reached. Elimination of W gives the following solution in the conjugated features,

$$\frac{1}{\eta}KH^T = H^T \Lambda, \tag{3.27}$$

where $H = [h_1 \dots h_N] \in \mathbb{R}^{s \times N}$ and $\Lambda = \text{diag}\{\lambda_1, \dots, \lambda_s\}$ with $s \leq N$ the number of selected components. One can verify that the solutions corresponding to the different eigenvectors h_i and their corresponding eigenvalues λ_i all lead to the value $J = 0$.

The primal and dual model representations are

$$\begin{array}{c} (P)_{\text{RKM}} : \hat{e} = W^T \varphi(x) \\ \nearrow \\ \mathcal{M} \\ \searrow \\ (D)_{\text{RKM}} : \hat{e} = \frac{1}{\eta} \sum_j h_j K(x_j, x). \end{array} \tag{3.28}$$

Here the number of hidden units equals s with $h \in \mathbb{R}^s$ and the visible units $v \in \mathbb{R}^{n_f}$ with $v = \varphi(x)$, and $R_{\text{RKM}}(v, h) = -v^T W h$.

3.5 Singular Value Decomposition. For the SVD case, we start from the objective in equation 2.17 and introduce the conjugated hidden features.

The model is characterized now by matrices W, V :

$$\begin{aligned}
 J &= -\frac{\eta}{2} \text{Tr}(V^T W) + \frac{1}{2\lambda} \sum_{i=1}^N e_i^T e_i + \frac{1}{2\lambda} \sum_{j=1}^M r_j^T r_j \\
 &\text{s.t. } e_i = W^T \varphi(x_i), \forall i \text{ \& } r_j = V^T \psi(z_j), \forall j \\
 &\geq \sum_{i=1}^N e_i^T h_{e_i} - \frac{\lambda}{2} \sum_{i=1}^N h_{e_i}^T h_{e_i} + \sum_{j=1}^M r_j^T h_{r_j} - \frac{\lambda}{2} \sum_{j=1}^M h_{r_j}^T h_{r_j} - \frac{\eta}{2} \text{Tr}(V^T W) \\
 &\text{s.t. } e_i = W^T \varphi(x_i), \forall i \text{ \& } r_j = V^T \psi(z_j), \forall j \\
 &= \sum_{i=1}^N \varphi(x_i)^T W h_{e_i} - \frac{\lambda}{2} \sum_{i=1}^N h_{e_i}^T h_{e_i} + \sum_{j=1}^M \psi(z_j)^T V h_{r_j} \\
 &\quad - \frac{\lambda}{2} \sum_{j=1}^M h_{r_j}^T h_{r_j} - \frac{\eta}{2} \text{Tr}(V^T W) \triangleq \underline{J}. \tag{3.29}
 \end{aligned}$$

In this case, $R_{\text{RKM}}^{\text{train}} = \sum_{i=1}^N \varphi(x_i)^T W h_{e_i} + \sum_{j=1}^M \psi(z_j)^T V h_{r_j}$. The stationary points of $\underline{J}(h_{e_i}, W, h_{r_j}, V)$ are given by

$$\begin{cases}
 \frac{\partial \underline{J}}{\partial h_{e_i}} = 0 \Rightarrow W^T \varphi(x_i) = \lambda h_{e_i}, \forall i \\
 \frac{\partial \underline{J}}{\partial W} = 0 \Rightarrow V = \frac{1}{\eta} \sum_i \varphi(x_i) h_{e_i}^T \\
 \frac{\partial \underline{J}}{\partial h_{r_j}} = 0 \Rightarrow V^T \psi(z_j) = \lambda h_{r_j}, \forall j \\
 \frac{\partial \underline{J}}{\partial V} = 0 \Rightarrow W = \frac{1}{\eta} \sum_j \psi(z_j) h_{r_j}^T.
 \end{cases} \tag{3.30}$$

Elimination of W, V gives the solution in the conjugated dual features h_{e_i}, h_{r_j} :

$$\begin{bmatrix} 0 & \frac{1}{\eta} [\varphi(x_i)^T \psi(z_j)] \\ \frac{1}{\eta} [\psi(z_j)^T \varphi(x_i)] & 0 \end{bmatrix} \begin{bmatrix} H_e^T \\ H_r^T \end{bmatrix} = \begin{bmatrix} H_e^T \\ H_r^T \end{bmatrix} \Lambda, \tag{3.31}$$

with $H_e = [h_{e_1} \dots h_{e_N}] \in \mathbb{R}^{s \times N}$, $H_r = [h_{r_1} \dots h_{r_M}] \in \mathbb{R}^{s \times M}$ and $\Lambda = \text{diag}\{\lambda_1, \dots, \lambda_s\}$ with $s \leq N + M$ a specified number of nonzero eigenvalues.

The primal and dual model representations are

$$\begin{array}{l}
 \nearrow \\
 \mathcal{M} \\
 \searrow
 \end{array}
 \begin{array}{l}
 (P)_{\text{RKM}} : \hat{e} = W^T \varphi(x) \\
 \hat{r} = V^T \psi(z) \\
 \\
 (D)_{\text{RKM}} : \hat{e} = \frac{1}{\eta} \sum_j h_{r_j} \psi(z_j)^T \varphi(x) \\
 \hat{r} = \frac{1}{\eta} \sum_i h_{e_i} \varphi(x_i)^T \psi(z),
 \end{array}
 \tag{3.32}$$

which corresponds to matrix SVD in the case of linear compatible feature maps and if an additional compatibility condition holds (Suykens, 2016).

3.6 Kernel pmf. For the case of kernel probability mass function (kernel pmf) estimation (Suykens, 2013), we start from the objective

$$J = \sum_{i=1}^N (p_i - \varphi(x_i)^T w) h_i - \sum_{i=1}^N p_i + \frac{\eta}{2} w^T w
 \tag{3.33}$$

in the unknowns $w \in \mathbb{R}^{n_f}$, $p_i \in \mathbb{R}$, and $h_i \in \mathbb{R}$. Suykens (2013) explained how a similar formulation is related to the probability rule in quantum measurement for a complex valued model.

The stationary points are characterized by

$$\begin{cases}
 \frac{\partial J}{\partial h_i} = 0 \Rightarrow p_i = w^T \varphi(x_i), \forall i \\
 \frac{\partial J}{\partial w} = 0 \Rightarrow w = \frac{1}{\eta} \sum_i \varphi(x_i) h_i \\
 \frac{\partial J}{\partial p_i} = 0 \Rightarrow h_i = 1, \forall i.
 \end{cases}
 \tag{3.34}$$

The regularization constant η can be chosen to normalize $\sum_i p_i = 1$ ($p_i \geq 0$ is achieved by the choice of an appropriate kernel function), which gives then the kernel pmf obtained in Suykens (2013). This results in the representations

$$\begin{array}{c}
 (P)_{\text{RKM}} : p_i = w^T \varphi(x_i) \\
 \nearrow \\
 \mathcal{M} \\
 \searrow \\
 (D)_{\text{RKM}} : p_i = \frac{1}{\eta} \sum_j K(x_j, x_i).
 \end{array} \tag{3.35}$$

4 Deep Restricted Kernel Machines

In this section we couple different restricted kernel machines within a deep architecture. Several coupling configurations are possible at this point. We illustrate deep restricted kernel machines here for an architecture consisting of three levels. We discuss two configurations:

1. Two kernel PCA levels followed by an LS-SVM regression level
2. LS-SVM regression level followed by two kernel PCA levels

In the first architecture, the first two levels extract features that are used within the last level for classification or regression. Related types of architectures are stacked autoencoders (Bengio, 2009), where a pretraining phase provides a good initialization for training the deep neural network in the fine-tuning phase. The deep RKM will consider an objective function jointly related to the kernel PCA feature extractions and the classification or regression. We explain how the insights of the RKM kernel PCA representations can be employed for combined supervised training and feature selection. A difference with other methods is also that conjugated features are used within the layered architecture.

In the second architecture, one starts with regression and then lets two kernel PCA levels further act on the residuals. In this case connections will be shown with deep Boltzmann machines (Salakhutdinov, 2015; Salakhutdinov & Hinton, 2009) when considering the special case of linear feature maps, though for the RKMs in a nonprobabilistic setting.

4.1 Two Kernel PCA Levels Followed by Regression Level. We focus here on a deep RKM architecture consisting of three levels:

- Level 1 consists of kernel PCA with given input data x_i and is characterized by conjugated features $h_i^{(1)}$.
- Level 2 consists of kernel PCA by taking $h_i^{(1)}$ as input and is characterized by conjugated features $h_i^{(2)}$.
- Level 3 consists of LS-SVM regression on $h_i^{(2)}$ with output data y_i and is characterized by conjugated features $h_i^{(3)}$.

As predictive model is taken,

$$\begin{aligned}
 \hat{e}^{(1)} &= W_1^T \varphi_1(x), \\
 \hat{e}^{(2)} &= W_2^T \varphi_2(\Lambda_1^{-1} \hat{e}^{(1)}), \\
 \hat{y} &= W_3^T \varphi_3(\Lambda_2^{-1} \hat{e}^{(2)}) + b,
 \end{aligned}
 \tag{4.1}$$

evaluated at point $x \in \mathbb{R}^d$. The level 1 part has feature map $\varphi_1 : \mathbb{R}^d \rightarrow \mathbb{R}^{n_{f_1}}$, $W_1 \in \mathbb{R}^{n_{f_1} \times s^{(1)}}$; the level 2 part $\varphi_2 : \mathbb{R}^{n_{f_1}} \rightarrow \mathbb{R}^{n_{f_2}}$, $W_2 \in \mathbb{R}^{n_{f_2} \times s^{(2)}}$; and the level 3 part $\varphi_3 : \mathbb{R}^{n_{f_2}} \rightarrow \mathbb{R}^{n_{f_3}}$, $W_3 \in \mathbb{R}^{n_{f_3} \times p}$. Note that $\Lambda_1^{-1} \hat{e}^{(1)}$ and $\Lambda_2^{-1} \hat{e}^{(2)}$ (with $\hat{e}^{(1)} \in \mathbb{R}^{s^{(1)}}$, $\hat{e}^{(2)} \in \mathbb{R}^{s^{(2)}}$) are taken as input for levels 2 and 3, respectively, where Λ_1, Λ_2 denote the diagonal matrices with the corresponding eigenvalues. The latter is inspired by the property that for the uncoupled kernel PCA levels, the property $h_i = e_i/\lambda$ holds on the training data according to equation 3.26, which is then further extended to the out-of-sample case in equation 4.1.

The objective function in the primal is

$$J_{\text{deep,P}} = J_1 + J_2 + J_3
 \tag{4.2}$$

with

$$\begin{aligned}
 J_1 &= -\frac{1}{2\lambda_1} \sum_{i=1}^N e_i^{(1)T} e_i^{(1)} + \frac{\eta_1}{2} \text{Tr}(W_1^T W_1) \\
 J_2 &= -\frac{1}{2\lambda_2} \sum_{i=1}^N e_i^{(2)T} e_i^{(2)} + \frac{\eta_2}{2} \text{Tr}(W_2^T W_2) \\
 J_3 &= \frac{1}{2\lambda_3} \sum_{i=1}^N e_i^{(3)T} e_i^{(3)} + \frac{\eta_3}{2} \text{Tr}(W_3^T W_3)
 \end{aligned}
 \tag{4.3}$$

with $\hat{e}_i^{(1)} = W_1^T \varphi_1(x_i)$, $\hat{e}_i^{(2)} = W_2^T \varphi_2(\Lambda_1^{-1} \hat{e}_i^{(1)})$, $\hat{y}_i = W_3^T \varphi_3(\Lambda_2^{-1} \hat{e}_i^{(2)}) + b$. However, this objective function is not directly usable for minimization due to the minus sign terms $-\frac{1}{2\lambda_1} \sum_{i=1}^N e_i^{(1)T} e_i^{(1)}$ and $-\frac{1}{2\lambda_2} \sum_{i=1}^N e_i^{(2)T} e_i^{(2)}$. For direct minimization of an objective in the primal, we will use the following stabilized version,

$$J_{\text{deep,P,stab}} = J_1 + J_2 + J_3 + \frac{1}{2} c_{\text{stab}} (J_1^2 + J_2^2),
 \tag{4.4}$$

with c_{stab} a positive constant. The role of this stabilization term for the kernel PCA levels is explained in the appendix. While in stacked autoencoders

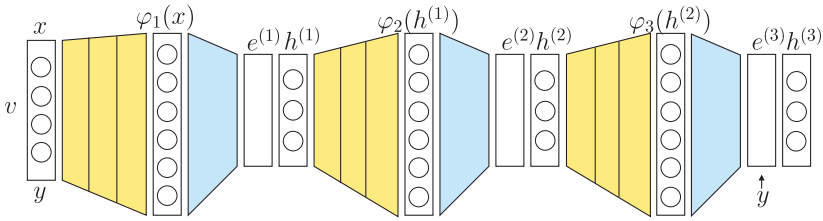


Figure 3: Example of a deep restricted kernel machine consisting of three levels with kernel PCA in levels 1 and 2 and LS-SVM regression in level 3.

one has an unsupervised pretraining and a supervised fine-tuning phase (Bengio, 2009), here we train the whole network at once.

For a characterization of the deep RKM in terms of the conjugated features $h_i^{(1)}, h_i^{(2)}, h_i^{(3)}$ (see Figure 3), we will study the stationary points of

$$J_{\text{deep}} = \bar{J}_1 + \bar{J}_2 + J_3, \tag{4.5}$$

where the objective $J_{\text{deep}}(h_i^{(1)}, W_1, h_i^{(2)}, W_2, h_i^{(3)}, W_3, b)$ for the deep RKM consists of the sum of the objectives of levels 1,2,3 given by $\bar{J}_1, \bar{J}_2, J_3$, respectively.

This becomes

$$\begin{aligned} J_{\text{deep}} = & - \sum_{i=1}^N \varphi_1(x_i)^T W_1 h_i^{(1)} + \frac{\lambda_1}{2} \sum_{i=1}^N h_i^{(1)T} h_i^{(1)} + \frac{\eta_1}{2} \text{Tr}(W_1^T W_1) \\ & - \sum_{i=1}^N \varphi_2(h_i^{(1)})^T W_2 h_i^{(2)} + \frac{\lambda_2}{2} \sum_{i=1}^N h_i^{(2)T} h_i^{(2)} + \frac{\eta_2}{2} \text{Tr}(W_2^T W_2) \\ & + \sum_{i=1}^N (y_i^T - \varphi_3(h_i^{(2)})^T W_3 - b^T) h_i^{(3)} \\ & - \frac{\lambda_3}{2} \sum_{i=1}^N h_i^{(3)T} h_i^{(3)} + \frac{\eta_3}{2} \text{Tr}(W_3^T W_3), \end{aligned} \tag{4.6}$$

with the following inner pairings at the three levels:

$$\text{Level 1 : } \sum_{i=1}^N e_i^{(1)T} h_i^{(1)} = \sum_{i=1}^N \varphi_1(x_i)^T W_1 h_i^{(1)},$$

$$\begin{aligned} \text{Level 2 : } & \sum_{i=1}^N e_i^{(2)T} h_i^{(2)} = \sum_{i=1}^N \varphi_2(h_i^{(1)})^T W_2 h_i^{(2)}, \\ \text{Level 3 : } & \sum_{i=1}^N e_i^{(3)T} h_i^{(3)} = \sum_{i=1}^N (y_i^T - \varphi_3(h_i^{(2)})^T W_3 - b^T) h_i^{(3)}. \end{aligned} \tag{4.7}$$

The stationary points of $J_{\text{deep}}(h_i^{(1)}, W_1, h_i^{(2)}, W_2, h_i^{(3)}, W_3, b)$ are given by

$$\left\{ \begin{aligned} \frac{\partial J_{\text{deep}}}{\partial h_i^{(1)}} = 0 & \Rightarrow W_1^T \varphi_1(x_i) = \lambda_1 h_i^{(1)} - \frac{\partial}{\partial h_i^{(1)}} [\varphi_2(h_i^{(1)})^T W_2 h_i^{(2)}], \quad \forall i, \\ \frac{\partial J_{\text{deep}}}{\partial W_1} = 0 & \Rightarrow W_1 = \frac{1}{\eta_1} \sum_i \varphi_1(x_i) h_i^{(1)T}, \\ \frac{\partial J_{\text{deep}}}{\partial h_i^{(2)}} = 0 & \Rightarrow W_2^T \varphi_2(h_i^{(1)}) = \lambda_2 h_i^{(2)} - \frac{\partial}{\partial h_i^{(2)}} [\varphi_3(h_i^{(2)})^T W_3 h_i^{(3)}], \quad \forall i, \\ \frac{\partial J_{\text{deep}}}{\partial W_2} = 0 & \Rightarrow W_2 = \frac{1}{\eta_2} \sum_i \varphi_2(h_i^{(1)}) h_i^{(2)T}, \\ \frac{\partial J_{\text{deep}}}{\partial h_i^{(3)}} = 0 & \Rightarrow y_i - W_3^T \varphi_3(h_i^{(2)}) - b = \lambda_3 h_i^{(3)}, \quad \forall i, \\ \frac{\partial J_{\text{deep}}}{\partial W_3} = 0 & \Rightarrow W_3 = \frac{1}{\eta_3} \sum_i \varphi_3(h_i^{(2)}) h_i^{(3)T}, \\ \frac{\partial J_{\text{deep}}}{\partial b} = 0 & \Rightarrow \sum_i h_i^{(3)} = 0. \end{aligned} \right. \tag{4.8}$$

The primal and dual model representations for the deep RKM are then

$$\begin{aligned} & \hat{e}^{(1)} = W_1^T \varphi_1(x) \\ (P)_{\text{DeepRKM}} : & \hat{e}^{(2)} = W_2^T \varphi_2(\Lambda_1^{-1} \hat{e}^{(1)}) \\ \nearrow & \hat{y} = W_3^T \varphi_3(\Lambda_2^{-1} \hat{e}^{(2)}) + b \\ \mathcal{M} & \\ \searrow & \hat{e}^{(1)} = \frac{1}{\eta_1} \sum_j h_j^{(1)} K_1(x_j, x) \\ (D)_{\text{DeepRKM}} : & \hat{e}^{(2)} = \frac{1}{\eta_2} \sum_j h_j^{(2)} K_2(h_j^{(1)}, \Lambda_1^{-1} \hat{e}^{(1)}) \\ & \hat{y} = \frac{1}{\eta_3} \sum_j h_j^{(3)} K_3(h_j^{(2)}, \Lambda_2^{-1} \hat{e}^{(2)}) + b. \end{aligned} \tag{4.9}$$

By elimination of W_1, W_2, W_3 , one obtains the following set of nonlinear equations in the conjugated features $h_i^{(1)}, h_i^{(2)}, h_i^{(3)}$ and b :

$$\left\{ \begin{aligned} \frac{1}{\eta_1} \sum_j h_j^{(1)} K_1(x_j, x_i) &= \lambda_1 h_i^{(1)} - \frac{1}{\eta_2} \sum_j \frac{\partial K_2(h_i^{(1)}, h_j^{(1)})}{\partial h_i^{(1)}} h_j^{(2)T} h_i^{(2)}, \forall i \\ \frac{1}{\eta_2} \sum_j h_j^{(2)} K_2(h_j^{(1)}, h_i^{(1)}) &= \lambda_2 h_i^{(2)} - \frac{1}{\eta_3} \sum_j \frac{\partial K_3(h_i^{(2)}, h_j^{(2)})}{\partial h_i^{(2)}} h_j^{(3)T} h_i^{(3)}, \forall i, \\ y_i &= \frac{1}{\eta_3} \sum_j h_j^{(3)} K_3(h_j^{(2)}, h_i^{(2)}) + b + \lambda_3 h_i^{(3)}, \forall i \\ \sum_i h_i^{(3)} &= 0. \end{aligned} \right. \tag{4.10}$$

Solving this set of nonlinear equations is computationally expensive. However, for the case of taking linear kernels K_2 and K_3 (and $K_{\text{lin}}, K_{2,\text{lin}}, K_{3,\text{lin}}$ denoting linear kernels) equation 4.10 simplifies to

$$\left\{ \begin{aligned} \text{Level 1 : } &\left(\frac{1}{\eta_1} [K_1(x_j, x_i)] + \frac{1}{\eta_2} [K_{\text{lin}}(h_j^{(2)}, h_i^{(2)})] \right) H_1^T = H_1^T \Lambda_1 \\ \text{Level 2 : } &\left(\frac{1}{\eta_2} [K_{2,\text{lin}}(h_j^{(1)}, h_i^{(1)})] + \frac{1}{\eta_3} [K_{\text{lin}}(h_j^{(3)}, h_i^{(3)})] \right) H_2^T = H_2^T \Lambda_2 \\ \text{Level 3 : } &\left[\begin{array}{c|c} \frac{1}{\eta_3} [K_{3,\text{lin}}(h_j^{(2)}, h_i^{(2)})] + \lambda_3 I_N & \mathbf{1}_N \\ \hline \mathbf{1}_N^T & 0 \end{array} \right] \left[\begin{array}{c} H_3^T \\ b^T \end{array} \right] = \left[\begin{array}{c} Y^T \\ 0 \end{array} \right]. \end{aligned} \right. \tag{4.11}$$

Here we denote $H_1 = [h_1^{(1)} \dots h_N^{(1)}], H_2 = [h_1^{(2)} \dots h_N^{(2)}], H_3 = [h_1^{(3)} \dots h_N^{(3)}]$. One sees that at levels 1 and 2, a data fusion is taking place between K_1 and K_{lin} and between $K_{2,\text{lin}}$ and K_{lin} , where $\frac{1}{\eta_1}, \frac{1}{\eta_2}, \frac{1}{\eta_3}$ are specifying the relative weight given to each of these kernels. In this way, one can choose for emphasizing or deemphasizing the levels with respect to each other.

4.2 Regression Level Followed by Two Kernel PCA Levels. In this case, we consider a deep RKM architecture with the following three levels:

- Level 1 consists of LS-SVM regression with given input data x_i and output data y_i and is characterized by conjugated features $h_i^{(1)}$.
- Level 2 consists of kernel PCA by taking $h_i^{(1)}$ as input and is characterized by conjugated features $h_i^{(2)}$.
- Level 3 consists of kernel PCA by taking $h_i^{(2)}$ as input and is characterized by conjugated features $h_i^{(3)}$.

We look then for the stationary points of

$$J_{\text{deep}} = \bar{J}_1 + \bar{J}_2 + \bar{J}_3 \tag{4.12}$$

where the objective $J_{\text{deep}}(h_i^{(1)}, W_1, b, h_i^{(2)}, W_2, h_i^{(3)}, W_3)$ for the deep RKM consists of the sum of the objectives of levels 1, 2, 3 given by $\bar{J}_1, \bar{J}_2, \bar{J}_3$, respectively. Deep RKM consists of coupling the RKMs.

This becomes

$$\begin{aligned} J_{\text{deep}} = & \sum_{i=1}^N (y_i^T - \varphi_1(x_i)^T W_1 - b^T) h_i^{(1)} - \frac{\lambda_1}{2} \sum_{i=1}^N h_i^{(1)T} h_i^{(1)} + \frac{\eta_1}{2} \text{Tr}(W_1^T W_1) \\ & - \sum_{i=1}^N \varphi_2(h_i^{(1)})^T W_2 h_i^{(2)} + \frac{\lambda_2}{2} \sum_{i=1}^N h_i^{(2)T} h_i^{(2)} + \frac{\eta_2}{2} \text{Tr}(W_2^T W_2) \\ & - \sum_{i=1}^N \varphi_3(h_i^{(2)})^T W_3 h_i^{(3)} + \frac{\lambda_3}{2} \sum_{i=1}^N h_i^{(3)T} h_i^{(3)} + \frac{\eta_3}{2} \text{Tr}(W_3^T W_3), \end{aligned} \tag{4.13}$$

with $\varphi_1 : \mathbb{R}^d \rightarrow \mathbb{R}^{n_{f_1}}$, $W_1 \in \mathbb{R}^{n_{f_1} \times p}$, the level 2 part $\varphi_2 : \mathbb{R}^p \rightarrow \mathbb{R}^{n_{f_2}}$, $W_2 \in \mathbb{R}^{n_{f_2} \times s^{(2)}}$, and the level 3 part $\varphi_3 : \mathbb{R}^{s^{(2)}} \rightarrow \mathbb{R}^{n_{f_3}}$, $W_3 \in \mathbb{R}^{n_{f_3} \times s^{(3)}}$. Note that in J_{deep} , the sum of the three inner pairing terms is similar to the energy in deep Boltzmann machines (Salakhutdinov, 2015; Salakhutdinov & Hinton, 2009) for the particular case of linear feature maps $\varphi_1, \varphi_2, \varphi_3$ and symmetric interaction terms. For the special case of linear feature maps, one has

$$U_{\text{deep}} = -v^T \tilde{W}_1 h^{(1)} - h^{(1)T} W_2 h^{(2)} - h^{(2)T} W_3 h^{(3)}, \tag{4.14}$$

which takes the same form as equation 29 in Salakhutdinov (2015), with \tilde{W}_1 defined in the sense of equation 3.1 in this letter. The “ U ” in U_{deep} refers to the fact that the deep RKM is unrestricted after coupling because of the hidden-to-hidden connections between layers 1 and 2 and between layers 2 and 3, while the uncoupled RKMs are restricted.

The stationary points of $J_{\text{deep}}(h_i^{(1)}, W_1, b, h_i^{(2)}, W_2, h_i^{(3)}, W_3)$ are given by

$$\left\{ \begin{aligned} \frac{\partial J_{\text{deep}}}{\partial h_i^{(1)}} = 0 &\Rightarrow y_i - W_1^T \varphi_1(x_i) - b = \lambda_1 h_i^{(1)} + \frac{\partial}{\partial h_i^{(1)}} \left[\varphi_2(h_i^{(1)})^T W_2 h_i^{(2)} \right], \forall i \\ \frac{\partial J_{\text{deep}}}{\partial W_1} = 0 &\Rightarrow W_1 = \frac{1}{\eta_1} \sum_i \varphi_1(x_i) h_i^{(1)T} \\ \frac{\partial J_{\text{deep}}}{\partial b} = 0 &\Rightarrow \sum_i h_i^{(1)} = 0 \\ \frac{\partial J_{\text{deep}}}{\partial h_i^{(2)}} = 0 &\Rightarrow W_2^T \varphi_2(h_i^{(1)}) = \lambda_2 h_i^{(2)} - \frac{\partial}{\partial h_i^{(2)}} \left[\varphi_3(h_i^{(2)})^T W_3 h_i^{(3)} \right], \forall i \\ \frac{\partial J_{\text{deep}}}{\partial W_2} = 0 &\Rightarrow W_2 = \frac{1}{\eta_2} \sum_i \varphi_2(h_i^{(1)}) h_i^{(2)T} \\ \frac{\partial J_{\text{deep}}}{\partial h_i^{(3)}} = 0 &\Rightarrow W_3^T \varphi_3(h_i^{(2)}) = \lambda_3 h_i^{(3)}, \forall i \\ \frac{\partial J_{\text{deep}}}{\partial W_3} = 0 &\Rightarrow W_3 = \frac{1}{\eta_3} \sum_i \varphi_3(h_i^{(2)}) h_i^{(3)T}. \end{aligned} \right. \quad (4.15)$$

As predictive model for this deep RKM case, we have

$$\begin{aligned} & (P)_{\text{DeepRKM}} : \hat{y} = W_1^T \varphi_1(x) + b \\ \mathcal{M} & \begin{matrix} \nearrow \\ \searrow \end{matrix} \\ & (D)_{\text{DeepRKM}} : \hat{y} = \frac{1}{\eta_1} \sum_j h_j^{(1)} K_1(x_j, x) + b. \end{aligned} \quad (4.16)$$

By elimination of W_1, W_2, W_3 , one obtains the following set of nonlinear equations in the conjugated features $h_i^{(1)}, h_i^{(2)}, h_i^{(3)}$, and b :

$$\left\{ \begin{aligned} y_i &= \frac{1}{\eta_1} \sum_j h_j^{(1)} K_1(x_j, x_i) + b + \lambda_1 h_i^{(1)} + \frac{1}{\eta_2} \sum_j \frac{\partial K_2(h_i^{(1)}, h_j^{(1)})}{\partial h_i^{(1)}} h_j^{(2)T} h_i^{(2)}, \forall i \\ \sum_i h_i^{(1)} &= 0 \\ \frac{1}{\eta_2} \sum_j h_j^{(2)} K_2(h_j^{(1)}, h_i^{(1)}) &= \lambda_2 h_i^{(2)} - \frac{1}{\eta_3} \sum_j \frac{\partial K_3(h_i^{(2)}, h_j^{(2)})}{\partial h_i^{(2)}} h_j^{(3)T} h_i^{(3)}, \forall i \\ \frac{1}{\eta_3} \sum_j h_j^{(3)} K_3(h_j^{(2)}, h_i^{(2)}) &= \lambda_3 h_i^{(3)}, \forall i. \end{aligned} \right. \quad (4.17)$$

When taking linear kernels K_2 and K_3 , the set of nonlinear equations simplifies to

$$\left\{ \begin{array}{l}
 \text{Level 1 : } \left[\begin{array}{c|c} \frac{1}{\eta_1}[K_1(x_j, x_i)] + \frac{1}{\eta_2}[K_{\text{lin}}(h_j^{(2)}, h_i^{(2)})] + \lambda_1 I_N & \mathbf{1}_N \\ \hline \mathbf{1}_N^T & 0 \end{array} \right] \begin{bmatrix} H_1^T \\ b^T \end{bmatrix} \\
 = \begin{bmatrix} Y^T \\ 0 \end{bmatrix} \\
 \text{Level 2 : } \left(\frac{1}{\eta_2}[K_{2,\text{lin}}(h_j^{(1)}, h_i^{(1)})] + \frac{1}{\eta_3}[K_{\text{lin}}(h_j^{(3)}, h_i^{(3)})] \right) H_2^T = H_2^T \Lambda_2 \\
 \text{Level 3 : } \left(\frac{1}{\eta_3}[K_{3,\text{lin}}(h_j^{(2)}, h_i^{(2)})] \right) H_3^T = H_3^T \Lambda_3
 \end{array} \right. \tag{4.18}$$

with a similar data fusion interpretation as explained in the previous subsection.

5 Algorithms for Deep RKM

The characterization of the stationary points for the objective functions in the different deep RKM models typically leads to solving large sets of nonlinear equations in the unknown variables, especially for large given data sets. Therefore, in this section, we outline a number of approaches and algorithms for working with the kernel-based models (in either the primal or the dual). We also outline algorithms for training deep feedforward neural networks in a parametric way in the primal within the deep RKM setting. The algorithms proposed in sections 5.2 and 5.3 are applicable also to large data sets.

5.1 Levelwise Solving for Kernel-Based Models. For the case of linear kernels in levels 2 and 3 in equation 4.11 and 4.18, we propose a heuristic algorithm that consists of level-wise solving linear systems and eigenvalue decompositions by alternating fixing different unknown variables.

For equation 4.18, in order to solve level 1 as a linear system, one needs the input/output data $X = [x_1 \dots x_N] \in \mathbb{R}^{d \times N}$, $Y = [y_1 \dots y_N] \in \mathbb{R}^{p \times N}$, but also the knowledge of $h_i^{(2)}$. Therefore, an initialization phase is required. One can initialize $h_i^{(2)}$ as zero or at random at level 1, obtain H_1 , and propagate it to level 2. At level 2, after initializing H_3 , one finds H_2 , which is then propagated to level 3, where one computes H_3 . After this forward phase, one can go backward from level 3 to level 1 in a backward phase.

Schematically this gives the following heuristic algorithm:

Forward phase (level 1 → level 3)

$$\begin{aligned}
 &H_2, H_3 \text{ initialization} \\
 \text{Level 1 : } &H_1 := f_1(X, Y, H_2) \text{ (for equation 4.18) or} \\
 &H_1 := f_1(X, H_2) \text{ (for equation 4.11)} \\
 \text{Level 2 : } &H_2 := f_2(H_1, H_3) \\
 \text{Level 3 : } &H_3 := f_3(H_2) \text{ (for equation 4.18) or} \\
 &H_3 := f_1(Y, H_2) \text{ (for equation 4.11)}
 \end{aligned} \tag{5.1}$$

Backward phase (level 3 → level 1)

$$\begin{aligned}
 \text{Level 2 : } &H_2 := f_2(H_1, H_3) \\
 \text{Level 1 : } &H_1 := f_1(X, Y, H_2) \text{ (for equation 4.18) or} \\
 &H_1 := f_1(X, H_2) \text{ (for equation 4.11)}.
 \end{aligned}$$

One can repeat the forward and backward phases a number of times, without the initialization step. Alternatively, one could also apply an algorithm with forward-only phases, which can then be applied a number of times after each other.

5.2 Deep Reduced Set Kernel-Based Models with Estimation in Primal. In the following approach, approximations $\tilde{W}_1, \tilde{W}_2, \tilde{W}_3$ are made to W_1, W_2, W_3 :

$$\begin{aligned}
 W_1 &= \frac{1}{\eta_1} \sum_{i=1}^N \varphi_1(x_i) h_i^{(1)T} \simeq \tilde{W}_1 = \frac{1}{\eta_1} \sum_{j=1}^M \varphi_1(\tilde{x}_j) \tilde{h}_j^{(1)T}, \\
 \tilde{W}_2 &= \frac{1}{\eta_2} \sum_{j=1}^M \varphi_2(\tilde{h}_j^{(1)}) \tilde{h}_j^{(2)T}, \\
 \tilde{W}_3 &= \frac{1}{\eta_3} \sum_{j=1}^M \varphi_2(\tilde{h}_j^{(2)}) \tilde{h}_j^{(3)T},
 \end{aligned} \tag{5.2}$$

where a subset of the training data set $\{\tilde{x}_j\}_{j=1}^M \subset \{x_i\}_{i=1}^N$ is considered with $M \ll N$. This approximation corresponds to a reduced-set technique in kernel methods (Schölkopf et al., 1999). In order to have a good representation of the data distribution, one can take a fixed-size algorithm with subset selection according to quadratic Renyi entropy (Suykens et al., 2002), or a random subset as a simpler scheme.

We proceed then with a primal estimation scheme by taking stabilization terms for the kernel PCA levels. In the case of two kernel PCA levels followed by LS-SVM regression, we minimize the following objective:

$$\begin{aligned}
 \min_{\tilde{h}_j^{(1)}, \tilde{h}_j^{(2)}, \tilde{h}_j^{(3)}, b, \Lambda_1, \Lambda_2} J_{\text{deep, Pstab}} = & -\frac{1}{2} \sum_{j=1}^M e_j^{(1)T} \Lambda_1^{-1} e_j^{(1)} \\
 & + \frac{\eta_1}{2} \text{Tr}(\tilde{W}_1^T \tilde{W}_1) - \frac{1}{2} \sum_{j=1}^M e_j^{(2)T} \Lambda_2^{-1} e_j^{(2)} \\
 & + \frac{\eta_2}{2} \text{Tr}(\tilde{W}_2^T \tilde{W}_2) + \frac{1}{2\lambda_3} \sum_{j=1}^M e_j^{(3)T} e_j^{(3)} + \frac{\eta_3}{2} \text{Tr}(\tilde{W}_3^T \tilde{W}_3) \\
 & + \frac{1}{2} c_{\text{stab}} \left(-\frac{1}{2} \sum_{j=1}^M e_j^{(1)T} \Lambda_1^{-1} e_j^{(1)} + \frac{\eta_1}{2} \text{Tr}(\tilde{W}_1^T \tilde{W}_1) \right)^2 \\
 & + \frac{1}{2} c_{\text{stab}} \left(-\frac{1}{2} \sum_{j=1}^M e_j^{(2)T} \Lambda_2^{-1} e_j^{(2)} + \frac{\eta_2}{2} \text{Tr}(\tilde{W}_2^T \tilde{W}_2) \right)^2. \tag{5.3}
 \end{aligned}$$

The predictive model then becomes:

$$\begin{aligned}
 \hat{e}^{(1)} &= \frac{1}{\eta_1} \sum_{j=1}^M \tilde{h}_j^{(1)} K_1(\tilde{x}_j, x), \\
 \hat{e}^{(2)} &= \frac{1}{\eta_2} \sum_{j=1}^M \tilde{h}_j^{(2)} K_2(\tilde{h}_j^{(1)}, \Lambda_1^{-1} \hat{e}^{(1)}), \\
 \hat{y} &= \frac{1}{\eta_3} \sum_{j=1}^M \tilde{h}_j^{(3)} K_3(\tilde{h}_j^{(2)}, \Lambda_2^{-1} \hat{e}^{(2)}) + b. \tag{5.4}
 \end{aligned}$$

The number of unknowns in this case is $M \times (s^{(1)} + s^{(2)} + p) + s^{(1)} + s^{(2)} + 1$. Alternatively, instead of the regularization terms $\text{Tr}(\tilde{W}_l^T \tilde{W}_l)$, one could also take $\text{Tr}(\tilde{H}^{(l)} \tilde{H}^{(l)T})$ where $\tilde{H}^{(l)} = [\tilde{h}_1^{(l)} \dots \tilde{h}_M^{(l)}]$ for $l = 1, 2, 3$.

One can also maximize $\text{Tr}(\Lambda_1) + \text{Tr}(\Lambda_2)$ by adding a term $-c_0(\text{Tr}(\Lambda_1) + \text{Tr}(\Lambda_2))$ to the objective, equation 5.3, with c_0 a positive constant. Note that the components of $\tilde{H}^{(1)}, \tilde{H}^{(2)}$ in levels 1 and 2 do not possess an orthogonality property unless this is imposed as additional constraints to the objective function.

5.3 Training Deep Feedforward Neural Networks within the Deep RKM Framework. For training of deep feedforward neural networks within this deep RKM setting, one minimizes $J_{\text{deep, P}_{\text{stab}}}$ in the unknown interconnection matrices of the different levels. In case one takes one hidden layer per level, the following objective is minimized

$$\begin{aligned}
 \min_{W_{1,2,3}, U_{1,2,3}, \beta_{1,2,3}, b, \Lambda_1, \Lambda_2} J_{\text{deep, P}_{\text{stab}}} &= -\frac{1}{2} \sum_{j=1}^M e_j^{(1)T} \Lambda_1^{-1} e_j^{(1)} \\
 &+ \frac{\eta_1}{2} \text{Tr}(W_1^T W_1) - \frac{1}{2} \sum_{j=1}^M e_j^{(2)T} \Lambda_2^{-1} e_j^{(2)} \\
 &+ \frac{\eta_2}{2} \text{Tr}(W_2^T W_2) + \frac{1}{2\lambda_3} \sum_{j=1}^M e_j^{(3)T} e_j^{(3)} + \frac{\eta_3}{2} \text{Tr}(W_3^T W_3) \\
 &+ \frac{1}{2} c_{\text{stab}} \left(-\frac{1}{2} \sum_{j=1}^M e_j^{(1)T} \Lambda_1^{-1} e_j^{(1)} + \frac{\eta_1}{2} \text{Tr}(W_1^T W_1) \right)^2 \\
 &+ \frac{1}{2} c_{\text{stab}} \left(-\frac{1}{2} \sum_{j=1}^M e_j^{(2)T} \Lambda_2^{-1} e_j^{(2)} + \frac{\eta_2}{2} \text{Tr}(W_2^T W_2) \right)^2 \tag{5.5}
 \end{aligned}$$

for the model

$$\begin{aligned}
 \hat{e}^{(1)} &= W_1^T \sigma(U_1 x + \beta_1), \\
 \hat{e}^{(2)} &= W_2^T \sigma(U_2 \Lambda_1^{-1} \hat{e}^{(1)} + \beta_2), \\
 \hat{y} &= W_3^T \sigma(U_3 \Lambda_2^{-1} \hat{e}^{(2)} + \beta_3) + b. \tag{5.6}
 \end{aligned}$$

Alternatively, one can take additional nonlinearities on $\Lambda_1^{-1} \hat{e}^{(1)}$, $\Lambda_2^{-1} \hat{e}^{(2)}$, which results in the model $\hat{e}^{(1)} = W_1^T \sigma(U_1 x + \beta_1)$, $\hat{e}^{(2)} = W_2^T \sigma(U_2 \sigma(\Lambda_1^{-1} \hat{e}^{(1)} + \beta_2))$, $\hat{y} = W_3^T \sigma(U_3 \sigma(\Lambda_2^{-1} \hat{e}^{(2)} + \beta_3) + b)$. The number of unknowns is $n_{h_1} \times (s^{(1)} + d + 1) + n_{h_2} \times (s^{(2)} + s^{(1)} + 1) + n_{h_3} \times (p + s^{(2)} + 1) + s^{(1)} + s^{(2)} + 1$, where $n_{h_{1,2,3}}$ denote the number of hidden units.

In order to further reduce the number of unknowns, and partially inspired by convolutional operations in convolutional neural networks (LeCun, Bottou, Bengio, & Haffner, 1998), we also consider the case where U_1 and U_2 are Toeplitz matrices. For a matrix $U \in \mathbb{R}^{n_1 \times n_2}$, the number of unknowns is reduced then from $n_1 n_2$ to $n_1 + n_2 - 1$.

Table 1: Comparison of Test Error (%) of Models \mathcal{M}_1 and \mathcal{M}_2 on UCI Data Sets.

| | pid | bld | ion | adu |
|-----------------------|----------------------------|----------------------------|-----------------------|----------------------|
| $\mathcal{M}_{1,a}$ | 19.53 [20.02(1.53)] | 26.09 [30.96(3.34)] | 0 [0.68(1.60)] | 16.99 [17.46(0.65)] |
| $\mathcal{M}_{1,b}$ | 18.75 [19.39(0.89)] | 25.22 [31.48(4.11)] | 0 [5.38(12.0)] | 17.08 [17.48(0.56)] |
| $\mathcal{M}_{1,c}$ | 21.88 [24.73(5.91)] | 28.69 [32.39(3.48)] | 0 [8.21(6.07)] | 17.83 [21.21(4.78)] |
| $\mathcal{M}_{2,a}$ | 21.09 [20.20(1.51)] | 27.83 [28.86(2.83)] | 1.71 [5.68(2.22)] | 15.07 [15.15(0.15)] |
| $\mathcal{M}_{2,b}$ | 18.75 [20.33(2.75)] | 28.69 [28.38(2.80)] | 10.23 [6.92(3.69)] | 14.91 [15.08 (0.15)] |
| $\mathcal{M}_{2,b,T}$ | 19.03 [19.16(1.10)] | 26.08 [27.74(9.40)] | 6.83 [6.50(8.31)] | 15.71 [15.97(0.07)] |
| $\mathcal{M}_{2,c}$ | 24.61 [22.34(1.95)] | 32.17 [27.61(3.69)] | 3.42 [9.66(6.74)] | 15.21 [15.19(0.08)] |
| bestbmark | 22.7(2.2) | 29.6(3.7) | 4.0(2.1) | 14.4(0.3) |

Notes: Shown first is the test error corresponding to the selected model with minimal validation error from the different random initializations. Between brackets, the mean and standard deviation of the test errors related to all initializations are shown. The lowest test error is in bold.

6 Numerical Examples

6.1 Two Kernel PCA Levels Followed by Regression Level: Examples.

We define the following models and methods for comparison:

- [\mathcal{M}_1]: *Deep reduced set kernel-based models* (with RBF kernel) with estimation in the primal according to equation 5.3 with the following choices:
 - $[\mathcal{M}_{1,a}]$: with additional term $-c_0(\text{Tr}(\Lambda_1) + \text{Tr}(\Lambda_2))$ and $\text{Tr}(\tilde{H}^{(l)}\tilde{H}^{(l)T})$ ($l = 1, 2, 3$) regularization terms
 - $[\mathcal{M}_{1,b}]$: without additional term $-c_0(\text{Tr}(\Lambda_1) + \text{Tr}(\Lambda_2))$
 - $[\mathcal{M}_{1,c}]$: with objective function $\frac{1}{2\lambda_3} \sum_{j=1}^M e_j^{(3)T} e_j^{(3)} + \frac{\eta_3}{2} \text{Tr}(W_3^T W_3)$, that is, only the level 3 regression objective.
- [\mathcal{M}_2]: *Deep feedforward neural networks* with estimation in the primal according to equation 5.5 with the same choices in [$\mathcal{M}_{2,a}$], [$\mathcal{M}_{2,b}$], [$\mathcal{M}_{2,c}$] as above in [\mathcal{M}_1]. In the model [$\mathcal{M}_{2,b,T}$] Toeplitz matrices are taken for the U matrices in all levels, except for the last level.

We test and compare the proposed algorithms on a number of UCI data sets: Pima indians diabetes (**pid**) ($d = 8, p = 1, N = 400, N_{\text{val}} = 112, N_{\text{test}} = 256$), Bupa liver disorder (**bld**) ($d = 6, p = 1, N = 170, N_{\text{val}} = 60, N_{\text{test}} = 115$), Johns Hopkins University ionosphere (**ion**) ($d = 34, p = 1, N = 170, N_{\text{val}} = 64, N_{\text{test}} = 117$), adult (**adu**) ($d = 14, p = 1, N = 22000, N_{\text{val}} = 11000, N_{\text{test}} = 12222$) data sets, where the number of inputs (d), outputs (p), training (N), validation (N_{val}), and test data (N_{test}) are indicated. These numbers correspond to previous benchmarking studies in Van Gestel et al. (2004). In Table 1, *bestbmark* indicates the best result obtained in the benchmarking study of Van Gestel et al. (2004) from different classifiers, including SVM and LS-SVM classifiers with linear, polynomial, and RBF kernel;

linear and quadratic discriminant analysis; decision tree algorithm C4.5; logistic regression; one-rule classifier; instance-based learners; and Naive Bayes.

The tuning parameters, selected at the validation level, are

- **pid**: For \mathcal{M}_1 : $s^{(1),(2),(3)} = 2, 2, p$; $M = 20$; $\lambda_3 = 10^{-2}$; $c_{\text{stab}} = 10$ ($\mathcal{M}_{1,a,b}$); $c_0 = 0.1$ ($\mathcal{M}_{1,a}$). For \mathcal{M}_2 : $s^{(1),(2),(3)} = 4, 2, p$; $n_{h_{1,2,3}} = 3, 3, 3$; $\lambda_3 = 10^{-2}$; $c_{\text{stab}} = 10$ ($\mathcal{M}_{2,a,b}$); $c_0 = 0.1$ ($\mathcal{M}_{2,a}$). For $\mathcal{M}_{2,b,T}$: $s^{(1),(2),(3)} = 4, 4, p$; $n_{h_{1,2,3}} = 3, 3, 3$; $\lambda_3 = 10^{-2}$; $c_{\text{stab}} = 1$.
- **bld**: For \mathcal{M}_1 : $s^{(1),(2),(3)} = 3, 2, p$; $M = 20$; $\lambda_3 = 10^{-3}$; $c_{\text{stab}} = 100$ ($\mathcal{M}_{1,a,b}$); $c_0 = 0.1$ ($\mathcal{M}_{1,a}$). For \mathcal{M}_2 : $s^{(1),(2),(3)} = 4, 2, p$; $n_{h_{1,2,3}} = 3, 3, 5$; $\lambda_3 = 10^{-3}$; $c_{\text{stab}} = 1000$ ($\mathcal{M}_{2,a,b}$); $c_0 = 0.1$ ($\mathcal{M}_{2,a}$). For $\mathcal{M}_{2,b,T}$: $s^{(1),(2),(3)} = 4, 2, p$; $n_{h_{1,2,3}} = 3, 3, 5$; $\lambda_3 = 10^{-3}$; $c_{\text{stab}} = 1000$.
- **ion**: For \mathcal{M}_1 : $s^{(1),(2),(3)} = 3, 2, p$; $M = 30$; $\lambda_3 = 10^{-3}$; $c_{\text{stab}} = 100$ ($\mathcal{M}_{1,a,b}$); $c_0 = 0.1$ ($\mathcal{M}_{1,a}$). For \mathcal{M}_2 : $s^{(1),(2),(3)} = 3, 3, p$; $n_{h_{1,2,3}} = 3, 3, 3$; $\lambda_3 = 10^{-3}$; $c_{\text{stab}} = 1000$ ($\mathcal{M}_{2,a,b}$); $c_0 = 0.1$ ($\mathcal{M}_{2,a}$). For $\mathcal{M}_{2,b,T}$: $s^{(1),(2),(3)} = 3, 3, p$; $n_{h_{1,2,3}} = 3, 3, 3$; $\lambda_3 = 10^{-3}$; $c_{\text{stab}} = 1000$.
- **adu**: For \mathcal{M}_1 : $s^{(1),(2),(3)} = 20, 10, p$; $M = 15$; $\lambda_3 = 10^{-3}$; $c_{\text{stab}} = 10^{-4}$ ($\mathcal{M}_{1,a,b}$); $c_0 = 0.1$ ($\mathcal{M}_{1,a}$). For \mathcal{M}_2 : $s^{(1),(2),(3)} = 5, 2, p$; $n_{h_{1,2,3}} = 10, 5, 3$; $\lambda_3 = 10^{-7}$; $c_{\text{stab}} = 0.1$ ($\mathcal{M}_{2,a,b}$); $c_0 = 0.1$ ($\mathcal{M}_{2,a}$). For $\mathcal{M}_{2,b,T}$: $s^{(1),(2),(3)} = 5, 2, p$; $n_{h_{1,2,3}} = 10, 5, 3$; $\lambda_3 = 10^{-7}$; $c_{\text{stab}} = 10$, $\eta_{1,2,3} = 1, 1, 1$.

The other tuning parameters were selected as $\eta_{1,2,3} = 1, 1, 1$ for **pid**, **bld**, **ion** and $\eta_{1,2} = 10^3$, $\eta_3 = 10^{-3}$ for **adu**, unless specified differently above. In the \mathcal{M}_1 and \mathcal{M}_2 models, the $\tilde{H}^{(1),(2),(3)}$ matrices and the interconnection matrices were initialized at random according to a normal distribution with zero mean and standard deviation 0.1 (100, 20, 10, and 3 initializations for **pid**, **bld**, **ion**, **adu**, respectively), the diagonal matrices $\Lambda_{1,2}$ by the identity matrix, and $\sigma_{1,2,3} = 1$ for the RBF kernel models in \mathcal{M}_1 . For the training, a quasi-Newton method was used with `fminunc` in Matlab.

The following general observations from the experiments are shown in Table 1:

- Having the additional terms with kernel PCA objectives in levels 1 and 2, as opposed to the level 3 objective only, gives improved results on all tried data sets.
- The best selected value for c_{stab} varies among the data sets. In case this value is large, the value of the objective function terms related to the kernel PCA parts is close to zero.
- The use of Toeplitz matrices for the U matrices in the deep feedforward neural networks leads to competitive performance results and greatly reduces the number of unknowns.

Figure 4 illustrates the evolution of the objective function (in logarithmic scale) during training on the **ion** data set, for different values of c_{stab} and in comparison with a level 3 objective function only.

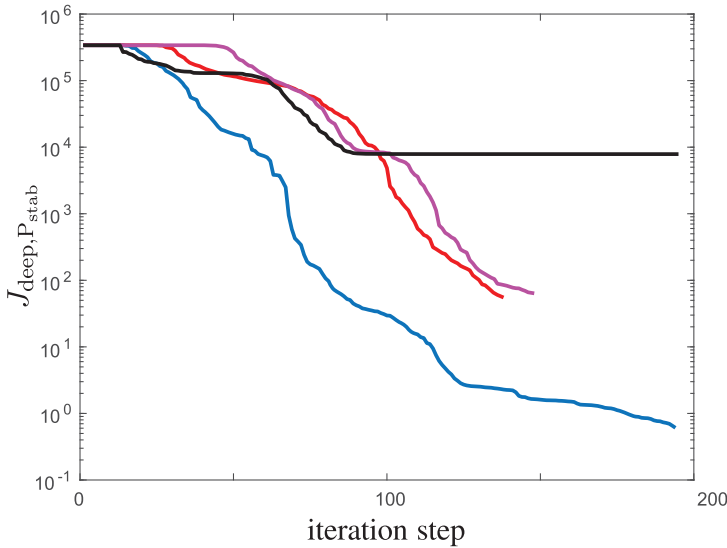


Figure 4: Illustration of the evolution of the objective function (logarithmic scale) during training on the ion data set. Shown are training curves for the model $\mathcal{M}_{2,a}$ for different choices of c_{stab} (equal to 1, 10, 100 in blue, red, and magenta, respectively) in comparison with $\mathcal{M}_{2,c}$ (level 3 objective only, in black), for the same initialization.

6.2 Regression Level Followed by Two Kernel PCA Levels: Examples.

6.2.1 Regression Example on Synthetic Data Set. In this example, we compare a basic LS-SVM regression with deep RKM consisting of three levels with LS-SVM + KPCA + KPCA, where a gaussian RBF kernel $K(x_i, x_j) = \exp(-\|x_i - x_j\|_2^2 / \sigma^2)$ is used in the LS-SVM level and linear kernels in the KPCA levels. Training, validation, and test data sets are generated from the following true underlying function,

$$f(x) = \sin(0.3x) + \cos(0.5x) + \sin(2x), \quad (6.1)$$

where zero mean gaussian noise with standard deviation 0.1, 0.5, 1, and 2 is added to the function values for the different data sets. In this example, we have a single input and single output $d = p = 1$. Training data (with noise) are generated in the interval $[-10, 10]$ with steps 0.1, validation data (with noise) in $[-9.77, 9.87]$ with steps 0.11, and test data (noiseless) in $[-9.99, 9.99]$ with steps 0.07. In the experiments, 100 realizations for the noise are made, for which the mean and standard deviation of the results are shown in Table 2. The tuning parameters are selected based on the

Table 2: Comparison between Basic LS-SVM Regression and Deep RKM on the Synthetic Data Set, for Different Noise Levels.

| Noise | Basic | Deep (1+1) | Deep (7+2) |
|-------|--------------------------------|--------------------------------|--------------------------------|
| 0.1 | $0.0019 \pm 4.3 \cdot 10^{-4}$ | $0.0018 \pm 4.2 \cdot 10^{-4}$ | $0.0019 \pm 4.4 \cdot 10^{-4}$ |
| 0.5 | 0.0403 ± 0.0098 | 0.0374 ± 0.0403 | 0.0397 ± 0.0089 |
| 1 | 0.1037 ± 0.0289 | 0.0934 ± 0.0269 | 0.0994 ± 0.0301 |
| 2 | 0.3368 ± 0.0992 | 0.2902 ± 0.0875 | 0.3080 ± 0.0954 |

validation set, which are σ, γ for the RBF kernel in the basic LS-SVM model and $\sigma, \lambda_1, \eta_2, \eta_3$ ($\eta_1 = 1$ has been chosen) for the complete deep RKM. The number of forward-backward passes in the deep RKM is chosen equal to 10. For deep RKM, we take the following two choices for the number of components $s^{(2)}, s^{(3)}$ in the KPCA levels: 1 and 1, 7 and 2 for level 2 and level 3, respectively. For deep RKM, the optimal values for $\frac{1}{\eta_2}, \frac{1}{\eta_3}$ are 10^5 , which means that the level 2 and 3 kernel PCA levels receive higher weight in the kernel fusion terms. As seen in Table 2, deep RKM improves over the basic LS-SVM regression in this example. The optimal values for (σ, λ_1) are (1, 0.001) for noise level 0.1 and (1, 0.01) for noise level 0.5, (1, 0.4) for noise level 1, and (1, 1) for noise level 2.

6.2.2 Multiclass Example: USPS. In this example, the USPS handwritten digits data set is taken from <http://www.cs.nyu.edu/~roweis/data.html>. It contains 8-bit grayscale images of digits 0 through 9 with 1100 examples of each class. These data are used without additional scaling or preprocessing. We compare a basic LS-SVM model (with primal representation $\hat{y} = W^T \varphi(x) + b$ and $W \in \mathbb{R}^{n_f \times p}, b \in \mathbb{R}^p$ with $p = 10$, that is, one output per class, and RBF kernel) with deep RKM consisting of LS-SVM + KPCA + KPCA with RBF kernel in levels 1 and linear kernels in levels 2 and 3 (with number of selected components $s^{(2)}, s^{(3)}$ in levels 2 and 3). In level 1 of deep RKM, the same type of model is taken as in the basic LS-SVM model. In this way, we intend to study the effect of the two additional KPCA layers. The dimensionality of the input data is $d = 256$. Two training set sizes were taken ($N = 2000$ and $N = 4000$ data points, that is, 200 and 400 examples per class), 2000 data points (200 per class) for validation, and 5000 data (500 per class) for testing. The tuning parameters are selected based on the validation set: σ, γ for the RBF kernel in the basic LS-SVM model and $\sigma, \lambda_1, \eta_2, \eta_3$ ($\eta_1 = 1$ has been chosen) for deep RKM. The number of forward-backward passes in the deep RKM is chosen equal to 2. The results are shown for the case of 2000 training data in Figure 5, showing the results on training, validation, and test data with the predicted class labels and the predicted output values for the different classes. For the case $N = 2000$, the selected values were $\sigma^2 = 45, s^{(2)} = 10, s^{(3)} = 1, \lambda_1 = 10^{-6}, \frac{1}{\eta_2} = \frac{1}{\eta_3} = 10^6$. The

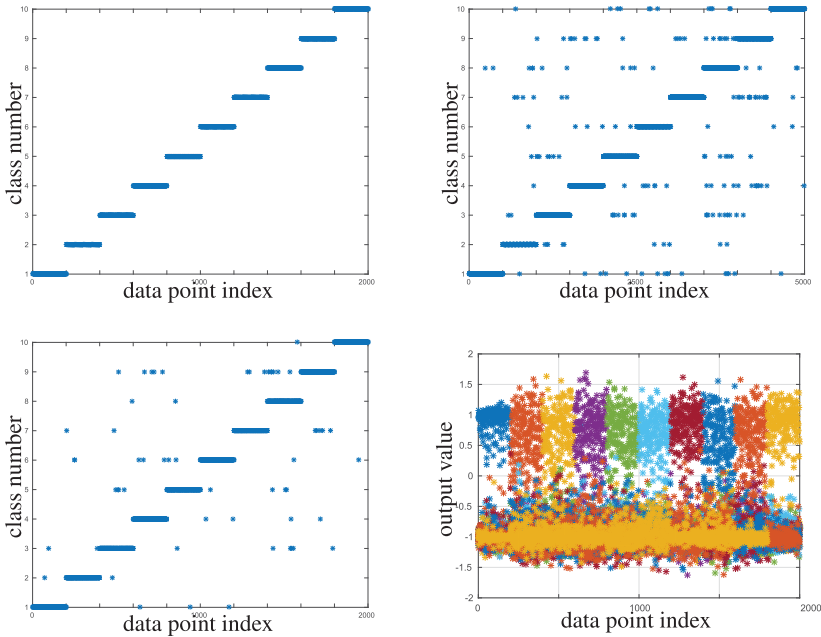


Figure 5: Deep RKM on USPS handwritten digits data set. Left top: Training data results (2000 data). Left Bottom: Validation data results (2000 data). Right top: Test data results (5000 data). Right bottom: Output values for the 10 different classes on the validation set.

misclassification error on the test data set is 3.18% for the deep RKM and 3.26% for the basic LS-SVM (with $\sigma^2 = 45$ and $\gamma = 1/\lambda_1$). For the case $N = 4000$, the selected values were $\sigma^2 = 45$, $s^{(2)} = 1$, $s^{(3)} = 1$, $\lambda_1 = 10^{-6}$, $\frac{1}{\eta_2} = \frac{1}{\eta_3} = 10^6$. The misclassification error on the test data set is 2.12% for the deep RKM and 2.14% for the basic LS-SVM (with $\sigma^2 = 45$ and $\gamma = 1/\lambda_1$). This illustrates that for deep RKM, levels 2 and 3 are given high relative importance through the selection of large $\frac{1}{\eta_2}$, $\frac{1}{\eta_3}$ values.

6.2.3 Multiclass Example: MNIST. The data set, which is used without additional scaling or preprocessing, is taken from <http://www.cs.nyu.edu/~roweis/data.html>. The dimensionality of the input data is $d = 784$ (images of size 28×28 for each of the 10 classes). In this case, we take an ensemble approach where the training set ($N = 50,000$ with 10 classes) has been partitioned into small nonoverlapping subsets of size 50 (5 data points per class). The choice for this subset size resulted from taking the last 10,000 points of this data set as validation data with the use of 40,000 data for training in that case. Other tuning parameters were selected in a similar way. The 1000 resulting submodels have been linearly combined

after applying the tanh function to their outputs. The linear combination is determined by solving an overdetermined linear system with ridge regression, following a similar approach as discussed in section 6.4 of Suykens et al. (2002). For the submodels, deep RKMs consisting of LSSVM + KPCA + KPCA with RBF kernel in levels 1 and linear kernels in levels 2 and 3, are taken. The selected tuning parameters are $\sigma^2 = 49$, $s^{(2)} = 1$, $s^{(3)} = 1$, $\lambda_1 = 10^{-6}$, $\eta_1 = 1$, $\frac{1}{\eta_2} = \frac{1}{\eta_3} = 10^{-6}$. The number of forward-backward passes in the deep RKM is chosen equal to 2. The training data set has been extended with another 50,000 training data consisting of the same data points but corrupted with noise (random perturbations with zero mean and standard deviation 0.5, truncated to the range [0,1]), which is related to the method with random perturbations in Kurakin, Goodfellow, and Bengio (2016). The misclassification error on the test data set (10,000 data points) is 1.28%, which is comparable in performance to deep belief networks (1.2%) and in between the reported test performances of deep Boltzmann machines (0.95, 1.01%) and SVM with gaussian kernel (1.4%) (Salakhutdinov, 2015) (see <http://yann.lecun.com/exdb/mnist/> for an overview and comparison of performances obtained by different methods).

7 Conclusion

In this letter, a theory of deep restricted kernel machines has been proposed. It is obtained by introducing a notion of conjugate feature duality where the conjugate features correspond to hidden features. Existing kernel machines such as least squares support vector machines for classification and regression, kernel PCA, matrix SVD, and Parzen-type models are considered as building blocks within a deep RKM and are characterized through the conjugate feature duality. By means of the inner pairing, one achieves a link with the energy expression of restricted Boltzmann machines, though with continuous variables in a nonprobabilistic setting. It also provides an interpretation of visible and hidden units. Therefore, this letter connects, on the one hand, to deep learning methods and, on the other hand, to least squares support vector machines and kernel methods. In this way, the insights and foundations achieved in these different research areas could possibly mutually reinforce each other in the future. Much future work is possible in different directions, including efficient methods and implementations for big data, the extension to other loss functions and regularization schemes, treating multimodal data, different coupling schemes, and models for clustering and semisupervised learning.

Appendix: Stabilization Term for Kernel PCA

We explain here the role of the stabilization term in kernel PCA as a modification to equation 2.15. In this case, the objective function in the primal is

$$\begin{aligned} \min_{w, e_i} \quad & \frac{1}{2} w^T w - \frac{\gamma}{2} \sum_i e_i^2 + \frac{c_{\text{stab}}}{2} \left(\frac{1}{2} w^T w - \frac{\gamma}{2} \sum_i e_i^2 \right)^2 \\ \text{subject to} \quad & e_i = w^T \varphi(x_i), \quad i = 1, \dots, N. \end{aligned} \quad (\text{A.1})$$

Denoting $J_0 = \frac{1}{2} w^T w - \frac{\gamma}{2} \sum_i e_i^2$ the Lagrangian is $\mathcal{L} = J_0 + \frac{c_{\text{stab}}}{2} J_0^2 + \sum_i \alpha_i (e_i - w^T \varphi(x_i))$, from which it follows that

$$\begin{cases} \frac{\partial \mathcal{L}}{\partial w} = 0 \Rightarrow (1 + c_{\text{stab}} J_0) w = \sum_i \alpha_i \varphi(x_i) \\ \frac{\partial \mathcal{L}}{\partial e_i} = 0 \Rightarrow (1 + c_{\text{stab}} J_0) \gamma e_i = \alpha_i \\ \frac{\partial \mathcal{L}}{\partial \alpha_i} = 0 \Rightarrow e_i = w^T \varphi(x_i). \end{cases}$$

Assuming that $1 + c_{\text{stab}} J_0 \neq 0$, elimination of w and e_i yields $\sum_j \alpha_j K_{ji} = (1/\gamma) \alpha_i$ with $K_{ji} = \varphi(x_j)^T \varphi(x_i)$, which is the solution that is also obtained for the original formulation (corresponding to $c_{\text{stab}} = 0$).

Acknowledgments

The research leading to these results has received funding from the European Research Council (FP7/2007-2013) / ERC AdG A-DATADRIVE-B (290923) under the European Union's Seventh Framework Programme. This letter reflects only my views; the EU is not liable for any use that may be made of the contained information; Research Council KUL: GOA/10/09 MaNet, CoE PFV/10/002 (OPTEC), BIL12/11T; PhD/Postdoc grants; Flemish government: FWO: PhD/postdoc grants, projects: G0A4917N (deep restricted kernel machines), G.0377.12 (Structured systems), G.088114N (tensor-based data similarity); IWT: PhD/postdoc grants, projects: SBO POM (100031); iMinds Medical Information Technologies SBO 2014; Belgian Federal Science Policy Office: IUAP P7/19 (DYSCO, dynamical systems, control and optimization, 2012–2017).

References

- Ackley, D. H., Hinton, G. E., & Sejnowski, T. J. (1985). A learning algorithm for Boltzmann machines. *Cognitive Science*, 9, 147–169.
- Alzate, C., & Suykens, J. A. K. (2010). Multiway spectral clustering with out-of-sample extensions through weighted kernel PCA. *IEEE Transactions on Pattern Analysis and Machine Intelligence*, 32(2), 335–347.
- Bengio, Y. (2009). *Learning deep architectures for AI*. Boston: Now.
- Bengio, Y., Courville, A., & Vincent, P. (2013). Representation learning: A review and new perspectives. *IEEE Transactions on Pattern Analysis and Machine Intelligence*, 35, 1798–1828.

- Boser, B. E., Guyon, I. M., & Vapnik, V. N. (1992). A training algorithm for optimal margin classifiers. In *Proceedings of the COLT Fifth Annual Workshop on Computational Learning Theory* (pp. 144–152). New York: ACM.
- Boyd, S., & Vandenberghe, L. (2004). *Convex optimization*. Cambridge: Cambridge University Press.
- Chen, L.-C., Schwing, A. G., Yuille, A. L., & Urtasun, R. (2015). Learning deep structured models. In *Proceedings of the 32nd International Conference on Machine Learning*.
- Cho, Y., & Saul, L. K. (2009). Kernel methods for deep learning. In Y. Bengio, D. Schuurmans, J. D. Lafferty, C. K. I. Williams, & A. Culotta (Eds.), *Advances in neural information processing systems*, 22. Red Hook, NY: Curran.
- Cortes, C., & Vapnik, V. (1995). Support vector networks. *Machine Learning*, 20, 273–297.
- Damianou, A. C., & Lawrence, N. D. (2013). Deep gaussian processes. *PMLR*, 31, 207–215.
- De Wilde, Ph. (1993). Class of Hamiltonian neural networks. *Phys. Rev. E*, 47, 1392–1396.
- Fischer, A., & Igel, C. (2014). Training restricted Boltzmann machines: An introduction. *Pattern Recognition*, 47, 25–39.
- Goldstein, H., Poole, C., & Safko, J. (2002). *Classical mechanics*. Reading, MA: Addison-Wesley.
- Golub, G. H., & Van Loan, C. F. (1989). *Matrix computations*. Baltimore: Johns Hopkins University Press.
- Goodfellow, I., Bengio, Y., & Courville, A. (2016). *Deep learning*. Cambridge, MA: MIT Press.
- Hertz, J., Krogh, A., & Palmer, R. G. (1991). *Introduction to the theory of neural computation*. Reading, MA: Addison-Wesley.
- Hinton, G. E. (2005). What kind of graphical model is the brain? In *Proc. 19th International Joint Conference on Artificial Intelligence* (pp. 1765–1775). San Francisco: Morgan Kaufmann.
- Hinton, G. E., Osindero, S., & Teh, Y.-W. (2006). A fast learning algorithm for deep belief nets. *Neural Computation*, 18, 1527–1554.
- Hopfield, J. J. (1982). Neural networks and physical systems with emergent collective computational abilities. *Proceedings of the National Academy of Sciences USA*, 79, 2554–2558.
- Jaderberg, M., Simonyan, K., Vedaldi, A., & Zisserman, A. (2015). Deep structured output learning for unconstrained text recognition. In *Proceedings of the International Conference on Learning Representations*.
- Kurakin, A., Goodfellow, I., & Bengio, S. (2016). *Adversarial machine learning at scale*. arXiv:1611.01236
- Larochelle, H., & Bengio, Y. (2008). Classification using discriminative restricted Boltzmann machines. In *Proceedings of the 25th International Conference on Machine Learning*. New York: ACM.
- LeCun, Y., Bengio, Y., & Hinton, G. (2015). Deep learning. *Nature*, 521, 436–444.
- LeCun, Y., Bottou, L., Bengio, Y., & Haffner, P. (1998). Gradient-based learning applied to document recognition. *Proceedings of the IEEE*, 86, 2278–2324.

- LeCun, Y., Chopra, S., Hadsell, R., Ranzato, M., & Huang, F.-J. (2006). A tutorial on energy-based learning. In G. Bakir, T. Hofmann, B. Schölkopf, A. Smola, & B. Taskar (Eds.), *Predicting structured data*. Cambridge, MA: MIT Press.
- Lee, H., Grosse, R., Ranganath, R., & Ng, A. Y. (2009). Convolutional deep belief networks for scalable unsupervised learning of hierarchical representations. In *Proceedings of the 26th Annual International Conference on Machine Learning* (pp. 609–616). New York: ACM.
- Mairal, J., Koniusz, P., Harchaoui, Z., & Schmid, C. (2014). Convolutional kernel networks. In Z. Ghahramani, M. Welling, C. Cortes, N. D. Lawrence, & K. Q. Weinberger (Eds.), *Advances in neural information processing systems* (NIPS).
- Mall, R., Langone, R., & Suykens, J. A. K. (2014). Multilevel hierarchical kernel spectral clustering for real-life large scale complex networks. *PLOS One*, 9(6), e99966.
- Petersen, K. B., & Pedersen, M. S. (2012). *The matrix cookbook*. Lyngby: Technical University of Denmark.
- Poggio, T., & Girosi, F. (1990). Networks for approximation and learning. *Proceedings of the IEEE*, 78(9), 1481–1497.
- Rasmussen, C. E., & Williams, C. (2006). *Gaussian processes for machine learning*. Cambridge, MA: MIT Press.
- Rockafellar, R. T. (1987). *Conjugate duality and optimization*. Philadelphia: SIAM.
- Rumelhart, D. E., Hinton, G. E., & Williams, R. J. (1986). Learning representations by back-propagating errors. *Nature*, 323, 533–536.
- Salakhutdinov, R. (2015). Learning deep generative models. *Annu. Rev. Stat. Appl.*, 2, 361–385.
- Salakhutdinov, R., & Hinton, G. E. (2007). Using deep belief nets to learn covariance kernels for gaussian processes. In J. Platt, D. Koller, Y. Singer, & S. T. Roweis (Eds.), *Advances in neural information processing systems*, 20. Red Hook, NY: Curran.
- Salakhutdinov, R., & Hinton, G. E. (2009). Deep Boltzmann machines. *PMLR*, 5, 448–455.
- Saunders, C., Gammerman, A., & Vovk, V. (1998). Ridge regression learning algorithm in dual variables. In *Proc. of the 15th Int. Conf. on Machine Learning* (pp. 515–521). San Francisco: Morgan Kaufmann.
- Schmidhuber, J. (2015). Deep learning in neural networks: An overview. *Neural Networks*, 61, 85–117.
- Schölkopf, B., Mika, S., Burges, C. C., Knirsch, P., Müller, K. R., Rätsch, G., & Smola, A. J. (1999). Input space versus feature space in kernel-based methods. *IEEE Transactions on Neural Networks*, 10(5), 1000–1017.
- Schölkopf, B., & Smola, A. (2002). *Learning with kernels*. Cambridge, MA: MIT Press.
- Schölkopf, B., Smola, A., & Müller, K.-R. (1998). Nonlinear component analysis as a kernel eigenvalue problem. *Neural Computation*, 10, 1299–1319.
- Schwing, A. G., & Urtasun, R. (2015). *Fully connected deep structured networks*. arXiv:1503.02351
- Smale, S., Rosasco, L., Bouvrie, J., Caponnetto, A., & Poggio, T. (2010). Mathematics of the neural response. *Foundations of Computational Mathematics*, 10(1), 67–91.
- Smolensky, P. (1986). Information processing in dynamical systems: Foundations of harmony theory. In D. E. Rumelhart & J. L. McClelland (Eds.), *Parallel distributed processing: Explorations in the microstructure of cognition*, vol. 1: *Foundations*. New York: McGraw-Hill.

- Srivastava, N., & Salakhutdinov, R. (2014). Multimodal learning with deep Boltzmann machines. *Journal of Machine Learning Research*, 15, 2949–2980.
- Stewart, G. W. (1993). On the early history of the singular value decomposition. *SIAM Review*, 35(4), 551–566.
- Suykens, J. A. K. (2013). Generating quantum-measurement probabilities from an optimality principle. *Physical Review A*, 87(5), 052134.
- Suykens, J. A. K. (2016). SVD revisited: A new variational principle, compatible feature maps and nonlinear extensions. *Applied and Computational Harmonic Analysis*, 40(3), 600–609.
- Suykens, J. A. K., Alzate, C., & Pelckmans, K. (2010). Primal and dual model representations in kernel-based learning. *Statistics Surveys*, 4, 148–183.
- Suykens, J. A. K., & Vandewalle, J. (1999a). Training multilayer perceptron classifiers based on a modified support vector method. *IEEE Transactions on Neural Networks*, 10(4), 907–911.
- Suykens, J. A. K., & Vandewalle, J. (1999b). Least squares support vector machine classifiers. *Neural Processing Letters*, 9(3), 293–300.
- Suykens, J. A. K., Vandewalle, J., & De Moor, B. (1995). *Artificial neural networks for modeling and control of non-linear systems*. New York: Springer.
- Suykens, J. A. K., Van Gestel, T., De Brabanter, J., De Moor, B., & Vandewalle, J. (2002). *Least squares support vector machines*. Singapore: World Scientific.
- Suykens, J. A. K., Van Gestel, T., Vandewalle, J., & De Moor, B. (2003). A support vector machine formulation to PCA analysis and its kernel version. *IEEE Transactions on Neural Networks*, 14(2), 447–450.
- Van Gestel, T., Suykens, J. A. K., Baesens, B., Viaene, S., Vanthienen, J., Dedene, G., De Moor, B., & Vandewalle, J. (2004). Benchmarking least squares support vector machine classifiers. *Machine Learning*, 54(1), 5–32.
- Vapnik, V. (1998). *Statistical learning theory*. New York: Wiley.
- Wahba, G. (1990). *Spline models for observational data*. Philadelphia: SIAM.
- Welling, M., Rosen-Zvi, M., & Hinton, G. E. (2004). Exponential family harmoniums with an application to information retrieval. In L. K. Saul, Y. Weiss, & L. Bottou (Eds.), *Advances in neural information processing systems*, 17. Cambridge, MA: MIT Press.
- Wiering, M. A., & Schomaker, L. R. B. (2014). Multi-layer support vector machines. In J. A. K. Suykens, M. Signoretto, & A. Argyriou (Eds.), *Regularization, optimization, kernels, and support vector machines* (pp. 457–476). Boca Raton, FL: Chapman & Hall/CRC.
- Zheng, S., Jayasumana, S., Romera-Paredes, B., Vineet, V., Su, Z., Du, D., Huang, C., & Torr, P. H. S. (2015). Conditional random fields as recurrent neural networks. In *Proceedings of the International Conference on Computer Vision*. Piscataway, NJ: IEEE.